Strength Behavior of Selected Asphalt-Aggregate Systems In Triaxial Compression

ANWAR E. Z. WISSA and SCOTT E. BLOUIN, Department of Civil Engineering, Massachusetts Institute of Technology

Some of the basic compositional and environmental factors influencing the strength behavior of asphaltic concrete are isolated and studied using consolidated-drained and consolidated-undrained triaxial compression tests. The factors include asphalt content, aggregate grain size and distribution, aggregate density, rate of strain, temperature, and volume change during shear.

It is shown that effective stresses rather than total stresses control the strength behavior of asphaltic concrete. The volume change behavior during shear is not only a function of the composition of the concrete but is also dependent on environmental factors such as temperature and rate of strain. Volumetric restraints during shear cause an increase in the strength of the concrete without altering the effective stress-strength parameters. For a given asphaltic concrete the magnitude of the volumetric strain during shear depends on the rate of strain and the temperature. Any theoretical model for asphaltic concrete should therefore take these effects into consideration.

The effective stress principle explains the effect of air void content on the strength of asphaltic concrete. The influence of changes in temperature on the effective stress-strength parameters suggests that optimum field compaction of asphaltic concrete may occur at temperatures below the maxima currently used in practice.

OVER the years the design of asphalt roads has been based on experience and empirical procedures. Today's higher tire pressures, higher speeds, and higher traffic volumes, along with the expenditure of large sums of money for the improvement of existing roads and construction of new ones, have necessitated a more thorough design procedure. The development of modern soil mechanics has greatly added to this knowledge, because a good foundation is essential to satisfactory pavement performance. However, the complicated strength properties of the bituminous carpet are not as easily defined. The great cost of faulty design necessitates a thorough investigation of these properties in the hope it will lead to a rational design procedure.

The bituminous carpet is made up of an asphalt cement binder and a mineral aggregate filler. The strength properties of this mix are derived from the qualities of both the binder and aggregate. They are influenced by time, temperature, rate of strain, confining pressure, type of binder, percentage of binder, aggregate material, aggregate gradation, aggregate angularity, amount of void space, and so forth. In addition, the carpet is subjected to a variety of loading conditions, ranging from a stationary vertical

Paper sponsored by Committee on Mechanical Properties of Bituminous Paving Mixtures and presented at the 47th Annual Meeting.

load, roughly equal to the tire inflation pressure, to double this vertical load applied over extremely short periods by moving vehicles. To further complicate this, horizontal shear force components resulting from the vertical may be as much as 60 percent of the vertical (10).

Field performance indicates that the most critical surface loading occurs during summer climatic conditions under heavy stationary loads, usually where heavy trucks are stopping and starting. These are likely to cause a plastic failure of the bituminous carpet.

The triaxial test is a logical means of testing bituminous material under conditions similar to those found to be critical in the field. It provides a method of determining the fundamental strength properties using the Mohr-Coulomb failure criterion, which is considered to be the most appropriate theory for analyzing the strength behavior of both cohesive and cohesionless particulate systems.

The purpose of this study was to investigate the basic strength properties of asphalt-aggregate systems using the triaxial compression test. By first studying the simplest system possible, asphalt combined with a single-sized perfectly spherical aggregate, it was hoped to isolate and define the effects of the many variables controlling the strength of the bituminous mixes.

LITERATURE REVIEW

Before attempting to obtain a fundamental understanding of the shear strength behavior of bituminous concrete mixes, we must understand the behavior of the aggregate filler without asphalt. This literature review summarizes some of the important theories on the shear strength behavior of particulate systems.

In recent years the triaxial test has been extensively used to study the strength behavior of cohesionless and cohesive soils, but its use for investigating the behavior of bituminous paving mixes has been limited. For the most part, bituminous paving mixes are designed empirically using past performance records rather than attempting a more scientific approach using complicated and often poorly defined strength parameters for asphaltic concrete. In a few instances researchers have attempted to determine the variables that control these parameters. Once the influence of the individual variables is clearly understood a start can be made toward the rational design of asphaltic concrete mixes.

Shear Strength of Particulate Systems

Mohr-Coulomb Criterion of Failure—The strength criterion most widely used today for particulate systems was first suggested by Coulomb (4), who used it to investigate the strength behavior of rocks and sands. He showed experimentally that the strength was made up of two physical components, which he measured separately. The first component, which he called "cohesion," he assumed was independent of the normal stress on the failure plane and was equal to the tensile strength of the material. The second component he assumed was directly proportional to the normal stress on the failure surface and, therefore, he called it "friction." He measured friction by determining the resistance to sliding between two surfaces of the materials as a function of normal stress. The Coulomb criterion of failure can be given by

$$s = c + \sigma_{ff} \tan \phi \qquad (1)$$

where

- s is the shear strength of the material,
- c is the cohesion,
- σ_{ff} is the normal stress on the failure plane at failure,
- ϕ is the angle of friction, and
- $\tan \phi$ is the coefficient of friction.

Coulomb also showed theoretically that the plane of minimum resistance (failure plane) was inclined at an angle of $45° + \phi/2$ to the major principal plane. Mohr later proposed a more general criterion of failure based on shear stress, which assumes that at failure the shear stress on the failure plane, τ_{ff}, and the normal stress on the failure plane, σ_{ff}, are uniquely related, i.e.,

$$\tau_{ff} = f(\sigma_{ff}) \tag{2}$$

and that the functional relation is a characteristic of the material that can be represented on a shear stress vs normal stress diagram by the envelope of all possible Mohr circles of stresses for the material.

When the functional relation of the Mohr criterion of failure is linear, it becomes identical to the Coulomb criterion of failure, i.e.,

$$\tau_{ff} = c + \sigma_{ff} \tan \phi \tag{3}$$

where

- c is the intercept of the Mohr-Coulomb envelope on the shear stress axis and is known as the cohesion intercept,
- $\tan \phi$ is the shape of the Mohr-Coulomb envelope and is known as the coefficient of internal friction, and
- ϕ is the angle of internal friction or the angle of shearing resistance.

The straight-line Mohr envelope given by Eq. 3 will be referred to as the Mohr-Coulomb envelope. The Mohr envelopes for most particulate systems are close to straight lines and therefore can usually be approximated by the Mohr-Coulomb equation. When the envelope is slightly curved an average straight line is used, but in such cases the stress range over which the approximation applies should be stated.

The Mohr criterion of failure assumes that failure is reached at point of first tangency with the Mohr envelope, which means that the failure surface is inclined at an angle of $45° + \phi/2$ to the major principal plane where ϕ is the angle whose tangent is the slope of the Mohr envelope at the point of first tangency.

Effective Stress Principle—In 1923 Terzaghi put forward the effective stress principle, which stated that the "effective" stress, $\bar{\sigma}$, controls the deformation behavior of saturated soils and that it is equal to the total stress (external stress) minus the pore water pressure, u, or, stated mathematically,

$$\bar{\sigma} = \sigma - u \tag{4}$$

In a discussion of a paper by Jürgenson (1934), Casagrande showed that the effective stress as defined by Eq. 4 also controls the strength behavior of particulate systems and that the Mohr-Coulomb envelope in terms of total stresses is not unique but dependent on the pore water conditions prior to and during shear.

If the Mohr-Coulomb envelope is plotted in terms of effective stresses, it is not appreciably influenced by drainage conditions nor the total stress path during triaxial compression. The Mohr-Coulomb criterion of failure for saturated particulate systems can therefore be rendered more unique if it is stated in terms of effective stresses, i.e.,

$$\tau_{ff} = \bar{c} + (\sigma_{ff} - u_f) \tan \phi \tag{5a}$$

or

$$\tau_{ff} = \bar{c} + \bar{\sigma}_{ff} \tan \phi \tag{5b}$$

where

τ_{ff} is the shear stress on the failure plane at failure*,
σ_{ff} is the total normal stress on the failure plane at failure*,
u_f is the pore water pressure at failure,
$\bar{\sigma}_{ff}$ is the effective normal stress on the failure plane at failures*,
$\bar{c}$ is the cohesion intercept in terms of effective stress (effective cohesion intercept), and
$\bar{\phi}$ is the angle of shearing resistance in terms of effective stress or angle of internal friction in terms of effective stress (effective angle of internal friction).

For saturated, unbound, particulate systems, the effective stress-strength parameters, $\bar{c}$ and $\bar{\phi}$, have been found to be approximately independent of drainage and/or volume change conditions. The Mohr-Coulomb criterion of failure in terms of effective stress is therefore considerably more useful than in terms of total stress, in which c and ϕ are completely dependent on testing conditions and may vary over a wide range. Further, the predicted orientation of the failure plane using $\bar{\phi}$ is in closer agreement with the observed failure surface than the orientation using ϕ.

Physical Significance of the Mohr-Coulomb Envelope—Rowe (14) has shown that for densely packed particulate cohesionless systems the shearing resistance in drained shear is made up of three components: one due to mineral-mineral friction, one due to geometric interference between particles, and one due to the work done during dilation. The mineral-mineral friction is related to the coefficient of sliding of a grain on a smooth surface of the same material. The shearing resistance due to dilation can be determined from the volume change vs axial strain curve. The particle-particle interlocking is dependent on the packing and shape of the grains.

In the case of a drained test on a dense particulate system, the maximum particle interlocking or interference occurs at a relatively small axial strain when the volume is a minimum. On further straining, the interlocking decreases because the volume starts increasing and it reaches a minimum at ultimate conditions when the volume has reached its maximum value. Rowe has shown that throughout dilation the change in packing occurs in such a way that the rate of internal work done by friction is a minimum. Therefore, the maximum principal stress difference occurs when the rate of volume change with axial strain is a maximum, i. e., at the point of inflection of the volume change vs axial strain curve. He showed theoretically that the effective principal stress ratio at peak strength and during subsequent state of deformation follows the law

$$\frac{\bar{\sigma}_1}{\bar{\sigma}_3} = \tan \alpha \tan (\phi_\mu + \beta) \tag{6}$$

where

$\bar{\sigma}_1$ is the major principal effective stress,
$\bar{\sigma}_3$ is the minor principal effective stress,
α is the angle between the plane of maximum interlocking of particles and the major principal plane,
β is the angle between the plane of sliding of the particle and the major principal plane, and
ϕ_μ is the angle of sliding friction of the particle on a smooth surface of the same material as the particles.

Rowe also showed that the energy ratio ($\dot{E}$) for fixed orientation of particle movement is given by

$$\dot{E} = \tan (\phi_\mu + \beta)/\tan \beta \tag{7}$$

*The orientation of the assumed failure plane with respect to the major principal plane is given by $\theta = 45° + \phi/2$ or $\bar{\theta} = 45° + \bar{\phi}/2$, but, since ϕ and $\bar{\phi}$ are not numerically the same, the orientation of the assumed failure plane will not be the same in terms of effective stress as in terms of total stress.

and, by differentiating Eq. 7, it can be shown that the rate of internal work done is a minimum when

$$\beta = 45° - \phi_\mu/2 \tag{8}$$

Rowe also showed that, for a number of different ideal packings of uniform particles,

$$\tan \alpha = (1 + d\dot{V}/\epsilon_1)/\tan \beta \tag{9}$$

where

$\dot{V}$ is the volumetric strain (volume increase being positive) = dV/V, and
ϵ_1 is the axial strain (compression being positive).

Rowe assumed that, since such a relation existed for a number of different ideal packings, it would also exist for a random packing. By substituting Eq. 8 and Eq. 9 in Eq. 6, he obtained

$$\frac{\bar{\sigma}_1}{\bar{\sigma}_3} = (1 + d\dot{V}/\epsilon_1) \tan^2 (45 + \phi_\mu/2) \tag{10}$$

It has been shown experimentally that Eq. 10 applies to densely-packed particulate systems as they approach failure during the first load application, and that on reloading the equation applies throughout shear. The stress-strain behavior of loose particulate systems deviates considerably from Eq. 10, especially during the first load application. As the number of load applications increases, the stress-strain behavior of a loose-packed system approaches that given by the equation. This is probably due to the fact that repeated loadings densify the system.

Considerable disagreement exists concerning the physical significance of the cohesion intercept and angle of shearing resistance as determined by the Mohr-Coulomb envelope. Wissa and Ladd (16) have shown that the Mohr-Coulomb effective cohesion intercept is a function of the strength of the cementation between particles, whereas the effective angle of internal friction is essentially independent of the cementation. They showed that for a uniform sand the cohesion intercept increased with increasing cement content and increasing curing time (strength of cementation), but the angle of internal friction was independent of the cementation and solely a function of the relative density of the sand excluding the cement.

According to Wissa and Ladd, the Mohr-Coulomb envelope represents conditions when the sum of the shearing resistance due to friction and the shearing resistance due to cohesion are a maximum. They show that, for particulate systems cemented with lime or portland cement, the maximum cohesive resistance occurs at a smaller shear strain and the maximum frictional resistance occurs at a larger shear strain than that required to reach the Mohr-Coulomb envelope. This type of cementation is not self-healing and therefore is partially destroyed by the time the Mohr-Coulomb envelope is reached, whereas a large relative movement between particles is needed to fully mobilize the friction and this only occurs after the Mohr-Coulomb envelope has been reached.

Shear Strength of Bituminous Mixes

Nijboer has done extensive research into the strength properties of bituminous concrete using the compression test. As is usual with triaxial test results, he uses the Mohr-Coulomb theory to separate the shear strength into two components: a cohesion term, c, which is stress independent and is equal to the shear intercept of the strength envelope, and a frictional term, which is directly proportional to the normal stress on the failure plane at failure. The constant of proportionality is known as the coefficient of internal friction, tan ϕ, and is equal to the slope of the failure envelope.

Nijboer finds that the angle of internal friction, ϕ, depends on the shape of the aggregate particles, with the angular particles giving higher values of ϕ. For a sandsheet mixture of river sand filler and asphalt he reported a ϕ of 28°, and for an asphaltic

concrete containing about 60 percent by weight of graded rock chippings, a ϕ of 35° (11, p. 39). Neither strain rate nor temperature had much effect on these friction angles.

For an asphaltic system using a one-size aggregate, the friction angle, ϕ, was not affected by changes in the particle diameter for either rounded or angular mixtures.

The sandsheet mixture without asphalt had a ϕ of 37.25°. With the addition of asphalt this dropped to 28°, indicating a lubrication effect of the asphalt as reported by Horsfield (7) and others. On the addition of rock chippings to this mixture, little effect on the friction angle was noticed until the percent by weight of chippings reached about 30°, then the friction angle rose to 35°. The addition of greater percentages of chippings had little additional effect. Nijboer hypothesizes that it takes about 30 percent chippings to form a skeleton of coarse aggregate which raises the friction angle.

There is little change in friction angle with changes in asphalt content except when so much asphalt is used that volume of voids falls to 2 percent of the total volume or less. At this point a drop in ϕ of about 10° for the asphaltic concrete and 7° for the sandsheet occurred. It was thought that during testing voids were lost and a hydrostatic pressure developed lowering the stresses between particles. Nijboer feels that this loss in frictional resistance is probably the most widespread cause of insufficient stability in road carpets.

Nijboer calls the cohesion intercept, c, the initial resistance and points out that it is very complicated in character. He assumes it is made up of various components. The first of these is termed the true interlock, τ_{hh}, and is due to the interlocking of angular components of the aggregate. The magnitude of τ_{hh} increases with the amount of angular particles in the mix, independent of size, and is also independent of the presence of asphalt. [In terms of effective stresses, interlocking only increases the frictional resistance but does not cause cohesion. In terms of total stresses an apparent cohesion can be observed but this is due to volume changes and pore pressures developed during shear.]

With a rounded aggregate system there is no true interlock and the initial resistance results from the asphaltic binder, which Nijboer termed τ_b; τ_b depends on the hardness of the binder and consequently on temperature, and is believed to be due to the resistance to shear of very thin layers of asphalt on the aggregate near the contact points. The number of contact points between aggregate particles, as measured by the ratio of filler to bituminous binder, has a marked effect on the value of τ_b.

The term τ_τ indicates the increase in initial resistance with the addition of coarse aggregate to a bituminous mix, and is proportional to τ_b.

While strain rate has little effect on ϕ, it is seen that total initial resistance increases with increasing strain rate. For a given asphalt, the effect of changing the asphalt penetration (by changing the test temperature) on initial resistance is negligible when penetration exceeds 50, but below a penetration of 50 the initial resistance increases rapidly with a decrease in penetration (a decrease in temperature).

Over the past 15 years an extensive triaxial test program on asphalt-aggregate mixes has been conducted at Purdue University directed toward the need for understanding the plastic deformation of these systems. It was run in the belief that Mohr's strength theory is more nearly in accordance with the behavior of bituminous mixtures than any of the other theories applicable to the strength properties of a cohesive-granular material.

Herrin and Goetz (6) made an investigation of aggregate shape on the stability of bituminous mixes. Variables studied included the shape of both coarse and fine aggregate and the grading of the aggregate. For a one-size gravel mixture, ϕ increased considerably with increasing angularity while c was not affected. As sample density increased, the effect of increasing the percentage of coarse gravel on increasing the strength lessened. At low densities, the increase from 0 to 55 percent of crushed (angular) gravel had little effect on ϕ while c increased slightly. Above 55 percent crushed aggregate, no further increase in c was observed.

At high densities, c and ϕ were not influenced by the percentage of crushed (angular) gravel over the full range from 0 to 100 percent. Finally, for both the high and low

densities, the cohesion was increased by changing the fine aggregate from rounded sand to crushed limestone, but ϕ was not affected appreciably.

Schaub and Goetz (15) conducted a study of the behavior of bituminous mixes using the triaxial cell with a device for measuring the volume change of the sample during shear. Since the void content is continuously changing during a test, it was felt that by monitoring the volume change the void content of a specimen could be evaluated at any given time. Their observations of volume-change characteristics are especially interesting since this investigation also studies the volume-change behavior during shear.

In measuring the volume change of an asphaltic concrete, a small decrease in volume occurred in all tests during the initial stages of the tests. Additional axial loading (stress controlled tests) produced a volume-change increase that continued to failure. Several explanations are given for the initial volume reduction. First, there may have been a recovery of expansion that occurred upon release of the compaction pressures applied during the sample fabrication. Second, there may have been an elastic compression of the specimens under the confining pressures. Third, there may have been plastic deformation of the bitumen.

The dilatancy portions of the volume change curves are explained by the fact that grains are forced to move apart to ride over one another. This expansion continues until all particles on the shear plane are free to move. At this point the maximum shear strength is reached. The dilatancy during shear occurs at a uniform rate with axial strain, the rate being a function of the initial density of the aggregate mass.

Between 0 and 2 percent axial strain, the magnitude of dilatancy increased with increasing compaction pressure (density) regardless of the asphalt content. At constant bulk density, the rate of volume increase with axial strain was greatest for the lower asphalt contents. It was felt that thicker films between the particles permitted greater strains with less particle movement.

Some relations between compactive effort (density) and cohesion were given for various asphalt contents. At both 3 and 4 percent asphalt content, the cohesion increased with increasing compactive efforts. At 5 percent it rose with increasing compactive effort, then dropped beyond the 400-psi effort. It was felt that beyond a critical value the bitumen forms thicker films on the aggregate particles causing a decrease in contact between them and a drop in the value of cohesion. However, the friction angle remains nearly constant over the range of compactive efforts investigated.

MATERIALS AND TESTING PROCEDURES

Only one asphalt was used throughout the test program. It was derived from Venezuela crude and had the following properties:

Penetration, 82-85	ASTM D 5-52
Softening point, 118 to 120 F	ASTM E 28-517
Viscosity, 9×10^7 cps at 70 F, 1×10^4 cps at 175 F	

To eliminate the system variables of grain size distribution and particle angularity, a single-sized spherical aggregate was used in the initial stages of testing. It consisted of nearly perfect spherical beads of crown-barium glass 0.278 mm in diameter.

In the later stages of testing, a well-graded glass-bead aggregate was used to study the effects of filler gradation on the strength properties. This consisted of the same crown-barium glass beads as used previously, ranging in size from No. 16 U. S. Standard sieve (1.19 mm) to No. 140 and finer (less than 0.105 mm). The gradation used was based on the equation by Fuller,

$$P = 100\sqrt{\frac{d}{D}}$$

where

P is the percent by weight passing a given sieve size,
d is the largest particle diameter passing that sieve size, and
D is the largest particle diameter.

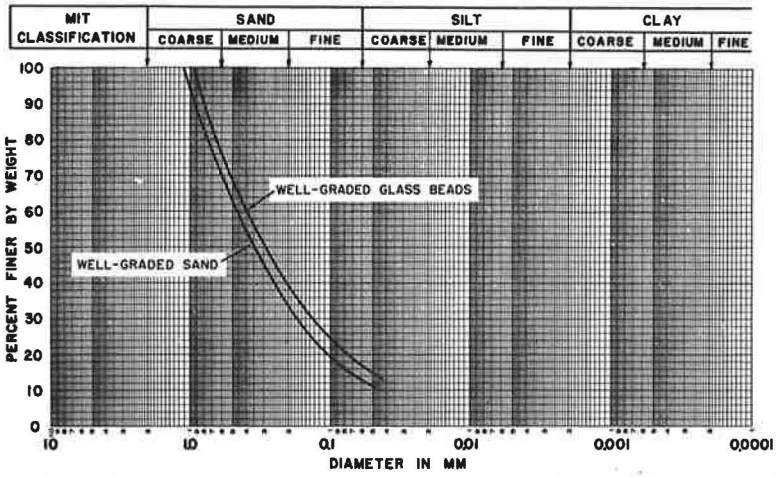

Figure 1. Grain size distribution of the well-graded glass beads and the well-graded quartz sand.

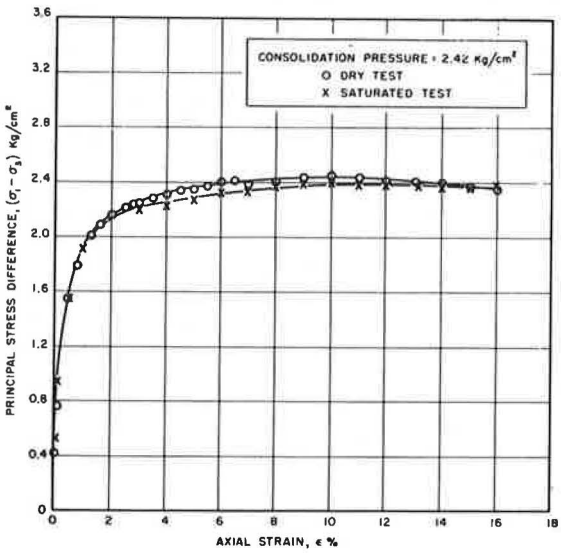

Figure 2. Influence of pore water on stress-strain curve for 0.278-mm beads plus 9 percent asphalt.

The grain size distribution is shown in Figure 1.

The final series of tests studied the behavior of a well-graded sand with and without asphalt. The graded sand consisted of a Fuller distribution of Ottawa sand and flint powder fines. Its grain size distribution (Fig. 1) closely resembled that used in the well-graded bead systems.

All test specimens were cylinders 3.15 in. long and 1.405 in. in diameter. The specimens containing asphalt were prepared in double-end static compaction while the specimens without asphalt were prepared on the triaxial cell base using the standard vacuum technique.

Triaxial Tests

Two types of triaxial compression tests were used in this investigation, consolidated-drained tests with volume-change measurements and consolidated-undrained tests with pore water pressure measurements. A brief description of these tests is given here; a detailed discussion appears elsewhere (19).

Consolidated-Drained Compression Tests—The consolidated-drained triaxial compression test with volume-change measurement was primarily used. In this test, the specimen is sealed to the base pedestal and top cap of the triaxial cell with a thin rubber membrane and O-rings. The specimen is then confined by a hydrostatic water pressure and is saturated by applying a pore water back pressure to the interior of the sample such that the difference between the two pressures is equal to the desired effective confining or consolidation pressure. The back pressure saturates the specimen by compressing the entrapped air and taking it into solution.

In the case of the Ottawa sand and asphalt system the permeability of the sample was so low that it could not be saturated with water. No back pressure was therefore used and the consolidation pressure was just equal to the cell pressure.

The test specimens were allowed to consolidate completely under the back pressure before shearing. The samples were sheared by increasing the axial load on the cell piston at a constant rate of strain. During shear the cell pressure and back pressure were kept constant at their initial values. The axial deformations of the test specimens were determined during shear using an Ames dial, which measured the piston travel. The total axial force applied to the cell piston was measured with a highly sensitive proving ring placed between the top of the piston and the loading frame. Volume changes during shear were measured in one of two ways. In all tests except the Ottawa sand series the volume change during shear was determined by measuring the flow of pore water into or out of the sample using a benzene type volume change apparatus having a resolution of 0.02 cc. To use this accurate method of measuring volume change it was necessary to have the pores of the specimens completely filled with water.

To check that saturation of the asphalt samples with water had no effect on the strength properties, tests were run on two identical samples of uniform 0.278-mm beads plus 9 percent asphalt at a bead density of 97.0 lb/cu ft. Each test was run at an effective confining pressure of 2.42 kg/cm^2. The first sample was saturated with water at a back pressure of 3.23 kg/cm^2 and tested at a cell pressure of 5.65 kg/cm^2. The second sample was run without water in the pores at a cell pressure of 2.42 kg/cm^2. The stress-strain curves are essentially identical, there being no more than a 3 percent separation at any strain, which is within experimental error. These results show that pore water in no way affects the strength of the samples (Fig. 2).

For the Ottawa sand and asphalt system, where the low sample porosity prevented saturation of the samples, the volume change during shear was determined by measuring the flow of water into or out of the cell chamber with the benzene type burrette. During shear the cell-water volume changes because of two factors: the volume change of the sample and the volume change of the cell chamber due to the movement of the cell piston and sealing diaphragm. The total volume change of the cell is recorded during shear and then corrected for the effect of the piston and diaphragm.

Consolidated-Undrained Compression Tests—The consolidated-undrained compression tests with pore pressure measurements were run on several duplicate samples of those used in the drained tests to determine the effect of restricting volume changes on the strength of the samples and to correlate volume change with excess pore pressure. The specimens were consolidated to an effective pressure of about 1 kg/cm^2 by using a cell pressure of 960 psi and back pressure of about 945 psi. These pressures necessitated use of specially designed high-pressure triaxial cells (19). After consolidation, the pore pressure lines were closed to prevent volume change of the specimens during shear. The high back pressure was needed to prevent cavitation of the pore water resulting from large negative excess pore pressures that developed during undrained shear. The pore pressure was continually measured using a diaphragm type millivolt pressure transducer.

Representation of Data

The shear stress on any plane in a sample during a triaxial compression test may be represented on the shear stress vs effective stress plot, τ vs $\bar{\sigma}$, by the locus of points forming a circle whose diameter is coincident with the $\bar{\sigma}$ axis between the points $\bar{\sigma}_3$, the effective confining pressure (cell pressure minus back pressure), and $\bar{\sigma}_1$, the effective axial load (stress due to the piston force plus the cell pressure minus the back pressure). When such a circle (a Mohr circle) becomes tangent to the failure envelope defined by Eq. 5b and known as the Mohr-Coulomb envelope, the sample is considered to have reached a failure condition (9).

Conversely, it is possible to determine the Mohr-Coulomb envelope by running drained triaxial compression tests at several different confining pressures. For each test, Mohr circles representing the stress history of the specimen during shear are constructed. A family of these circles is drawn for each consolidation pressure and an envelope is drawn tangent to all the families. The stress history of a specimen during shear can be more easily represented by an effective stress path, which is the locus of the stress history on a fixed plane. The failure plane is usually selected as

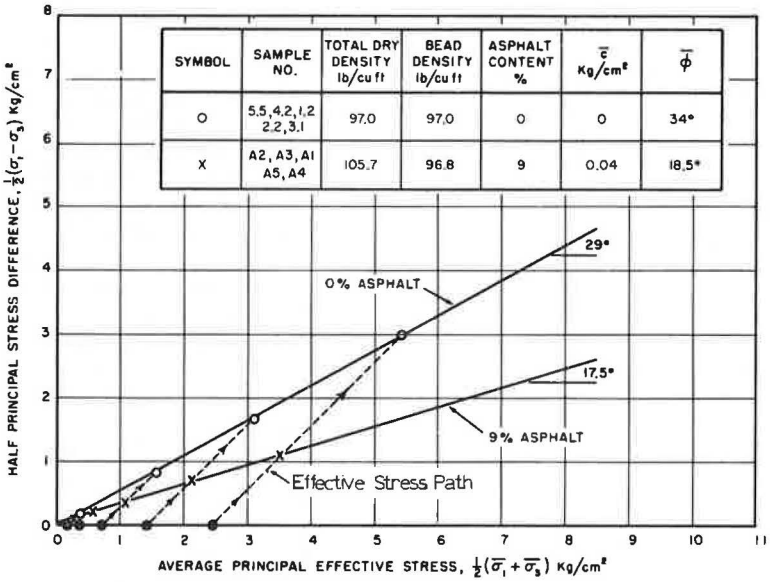

Figure 3. Influence of asphalt on the effective stress-strength behavior of 0.278-mm glass beads at 0.1 percent axial strain per min.

the fixed plane, but in this investigation the 45° plane was used to facilitate computations. The effective stress paths and effective stress-strength envelopes have therefore drawn on $\bar{p}$ vs q plots where $\bar{p} = 1/2\ (\bar{\sigma}_1 + \bar{\sigma}_3)$ and $q = 1/2\ (\bar{\sigma}_1 - \bar{\sigma}_3)$. A Mohr circle of stresses can easily be obtained for any point, $(\bar{p}, q)$, on such a plot by simply drawing through the point a circle whose radius is equal to the ordinate, q, and whose center lies on the $\bar{p}$ axis at a distance $\bar{p}$ from the origin.

The effective stress path that usually defines the stress history during shear on the plane at $45° + \bar{\phi}/2$ to the major principal plane (failure plane) is now the locus of stresses on the maximum shear plane, which is still a fixed plane with respect to the principal planes and is at an angle of 45° to them.

The trigonometric relations between the Mohr-Coulomb effective stress parameters, $\bar{c}$ and $\bar{\phi}$, and the q intercept, $\bar{a}$, and angle $\bar{\alpha}$ of the $\bar{p}$-q envelope are

$$\tan \bar{\alpha} = \sin \bar{\phi} \tag{11}$$

$$\bar{c} = \bar{a} \frac{\tan \bar{\phi}}{\tan \bar{\alpha}} = \frac{\bar{a}}{\cos \bar{\phi}} \tag{12}$$

The angle and intercept of the envelopes as obtained on the $\bar{p}$-q plots have been converted using the above relations and only the values of the effective stress parameters, $\bar{c}$ and $\bar{\phi}$, are referred to in this paper.

EXPERIMENTAL RESULTS

Compositional Factors

Asphalt Content—In order to determine the inflence of asphalt content on the strength behavior, consolidated-drained triaxial compression tests were run on four sets of samples having a bead density of 97 lb/cu ft and 0, 3, 6, and 9 percent asphalt contents by weight. All tests were run at a temperature of 21.0 ± 0.5 C with consolidation pressures ranging from 0.141 kg/cm^2 to 4.22 kg/cm^2. The tests on the plain bead samples and on the 9 percent asphalt samples were run at 0.1 percent strain per min.

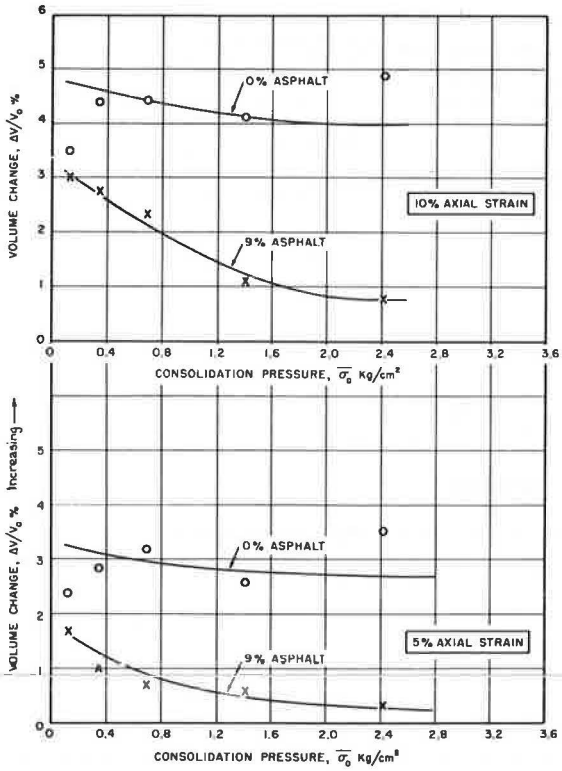

Figure 4. Influence of asphalt on the dilation of 0.278-mm glass beads.

To speed up testing, the 9 percent asphalt samples were rerun at 1.0 percent strain per min, as were the 6 and 3 percent asphalt samples. The tests on the untreated beads were not repeated because rate of strain does not affect the friction angle of a cohesionless granular system. The cohesion intercept of the 9 percent asphalt sample increased somewhat with the increase in strain rate, while the friction angle was not altered. This is discussed further in the section on influence of strain rate. During shear all samples bulged out around the center.

The Mohr-Coulomb envelopes for the plain bead system and the 9 percent asphalt and bead system at 0.1 percent strain per min are shown in Figure 3. The envelopes of the untreated and treated samples plotted as straight lines.

The effect of adding 9 percent asphalt to the untreated bead system while holding all other variables constant was to increase the effective cohesion, $\bar{c}$, from 0.0 to 0.04 kg/cm^2 and to decrease the effective angle of internal friction, $\bar{\phi}$, from 34° to 18.5°. Thus, asphalt seems to impart a cohesion to the samples and acts as a lubricant along the planes of failure. The asphalt coat on each particle acts like a lubricating oil lowering the coefficient of friction (tan ϕ_μ) between the glass beads and thus lowering $\bar{\phi}$ (see Eq. 10). Characteristically, the stress-strain curves for both systems rose sharply to a peak, the asphalt-bead curves then leveling off at a nearly constant value while the plain bead curves dropped off somewhat before reaching a constant value.

The volume-change curves were slightly negative for very small strains, indicating a slight initial volume decrease, but then rapidly became positive showing considerable dilation during shear. In all cases except at the lowest consolidation pressure, the dilation of the plain bead samples was much larger than that of the asphalt bead samples. According to Rowe (14), this indicates that the plain bead samples require a large input of energy to reach failure, which is due to a higher ϕ_μ as can be seen from Eqs. 7 and 8. The asphalt acts as a lubricant, permitting less total volume change during shear by allowing an easier and consequently more extensive movement of particles in the failure zone, resulting in an overall rise in the "efficiency" of the failure mechanism.

A slight volume decrease was observed with both the plain and asphalt samples during initial stages of shear, and this therefore is obviously a property of the granular material. It is evidently caused by the initial low shear stresses densifying the aggregate in the potential failure zone. The asphalt samples exhibited larger and more prolonged densification due to the lubricating effect of the asphalt.

Figure 4 is a plot of volume change vs consolidation pressure at two axial strains (10 and 5 percent). These plots show that the magnitude of volume change decreases as the effective confining pressure is increased. While the curves for the plain bead system in Figure 4 are not well defined, it can be seen that the decrease in volume with

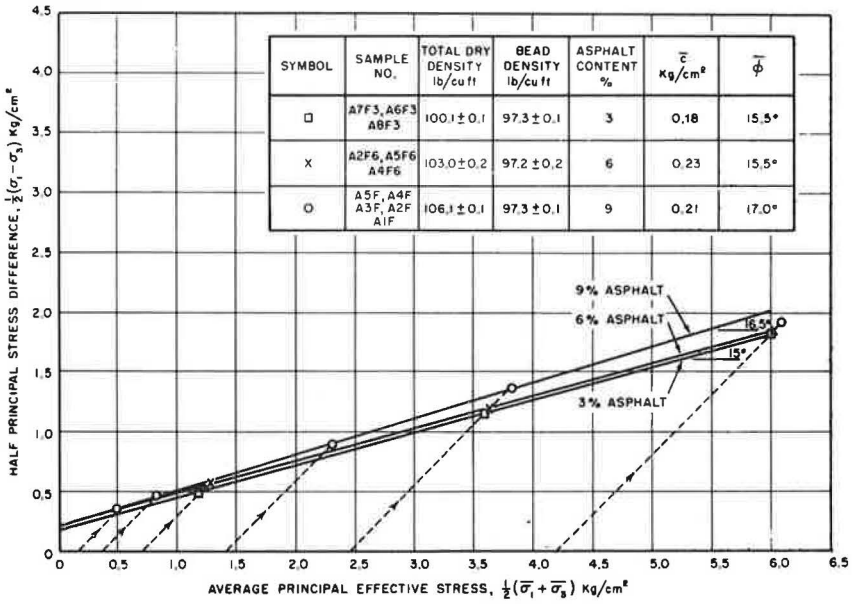

Figure 5. Influence of asphalt content on effective stress-strength behavior of 0.278-mm beads at a particle density of 97.3 lb/cu ft sheared at 1.0 percent axial strain per min.

increasing consolidation pressure is greater for the asphalt-bead system. This is again a consequence of the lubrication properties of the asphalt.

From Figure 5, it is seen that reducing the asphalt content of the samples from 9 to 6 to 3 percent had no significant effect on the strength parameters, $\bar{c}$ and $\bar{\phi}$. The only significant effect was on the volume change behavior. The samples with the higher asphalt contents experienced the larger dilations during shear. The addition of more asphalt to a sample at the same bead density deposits a thicker film of asphalt on the beads. This apparently causes increased volume change. The effect is like that of increasing the size of the glass beads without altering the asphalt film (lubricant) thickness. Thus, only an increased volume change results without a noticeable effect on the other parameters.

At some point below 3 percent asphalt content, the film coating the beads will become so thin that good lubrication between beads will no longer be provided. This would result in an increase in friction angle toward that of the plain beads.

Influence of Density—Two sets of samples with 0.278-mm beads and 9 percent asphalt were prepared at an average initial bead density of 92.7 and 99.2 lb/cu ft and tested over a range of consolidation pressures (0.703 kg/cm^2 to 4.22 kg/cm^2) at a strain rate of 1 percent/min and a temperature of 21 C. These densities were the maximum and minimum that could be readily reproduced in the laboratory. Although these densities do not differ by much, the shearing characteristics were very different. (It is interesting to note that the theoretical maximum density for single size glass spheres in a hexagonal close-packed array is 122 lb/cu ft, which is much higher than could be experimentally obtained.) The strength envelopes for the two systems are shown in Figure 6.

It is perhaps surprising that there was no significant difference in either the cohesions, 0.16 kg/cm^2 vs 0.23 kg/cm^2, or the friction angles, 16.0° vs 17.5°. It is evident from the typical stress-strain and volume-change plots shown in Figure 7 that, whereas the strength parameters are roughly equal, the failure mechanisms that determine these parameters are considerably different.

The stress-strain curves for the high-density samples rose sharply to a peak and then fell off slightly. The low-density samples, with the exception of that at the lowest

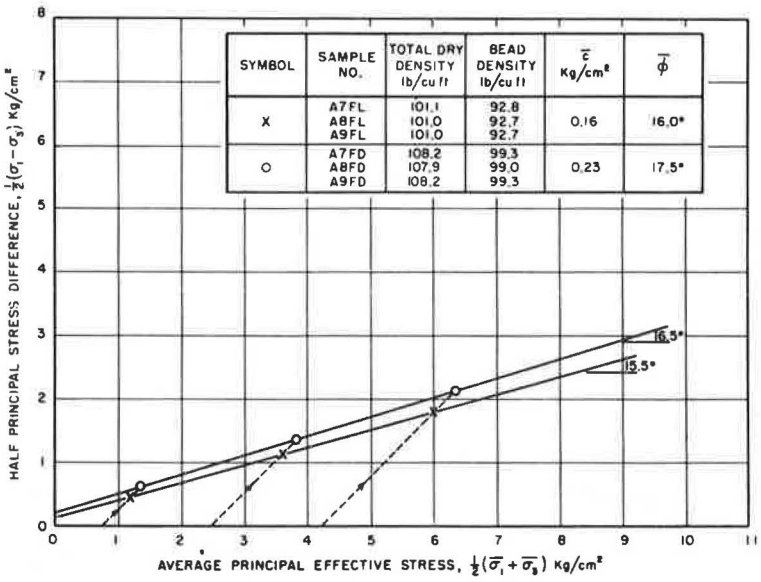

Figure 6. Influence of bead density on the effective stress-strength behavior of 0.278-mm beads with 9 percent asphalt sheared at 1.0 percent axial strain per min.

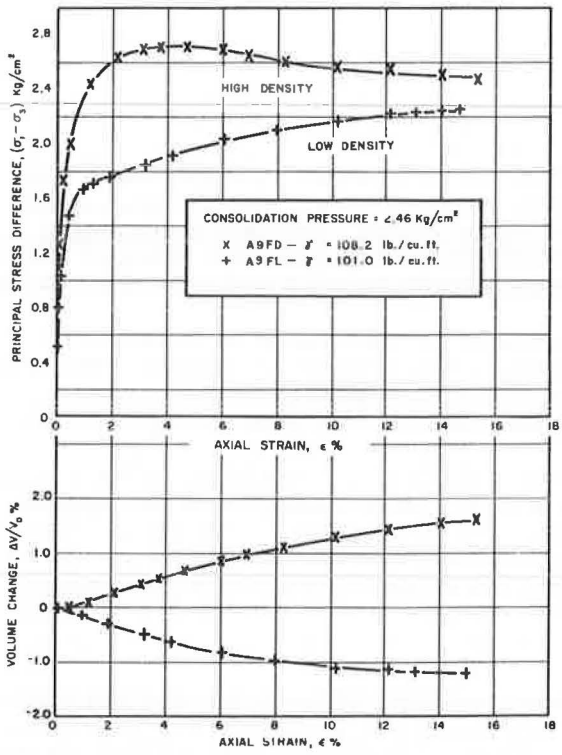

Figure 7. Influence of density on the stress-strain and volume change behavior of 0.278-mm beads plus 9 percent asphalt.

effective confining pressure, initially rose sharply but then bent over and continued to rise gradually throughout the remainder of the tests. At the termination of the tests these curves had risen nearly to the height of the high-density curves. In other words, the shear strength continued to build up throughout the tests. Since failure in consolidated-drained triaxial compression tests occurs at the maximum stress difference, it can be seen from the stress-strain curves that failure of the high-density samples occurred at about 4 percent strain, while the low-density samples failed at about 15 percent strain.

This stress-strain behavior can be explained by analyzing the volume change curves. The low-density samples at the higher consolidation pressures had an increasing negative volume change throughout the tests while the high-density samples were dilating. This tended to cause an equalization of the void ratios of the low- and high-density specimens in the shear zones by the time failure was reached. This phenomenon is known to occur in sands.

This influence of bead density on the dilation of the 0.278-mm beads with

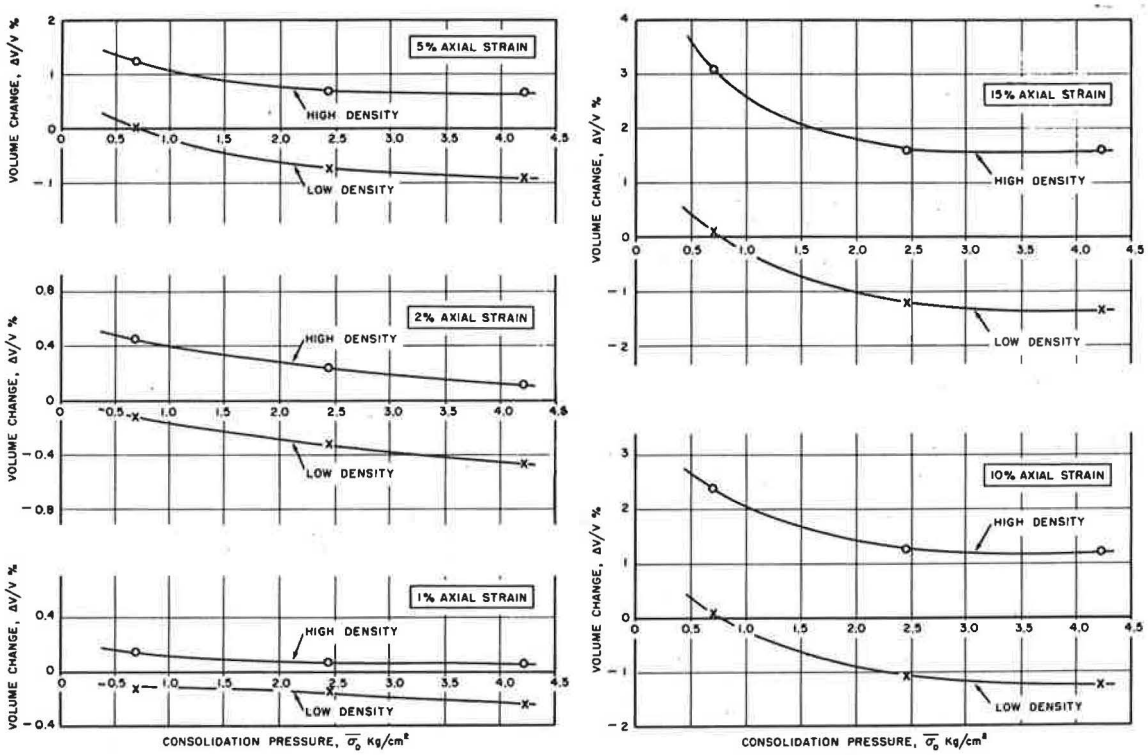

Figure 8. Influence of density on the dilation of 0.278-mm beads plus 9 percent asphalt.

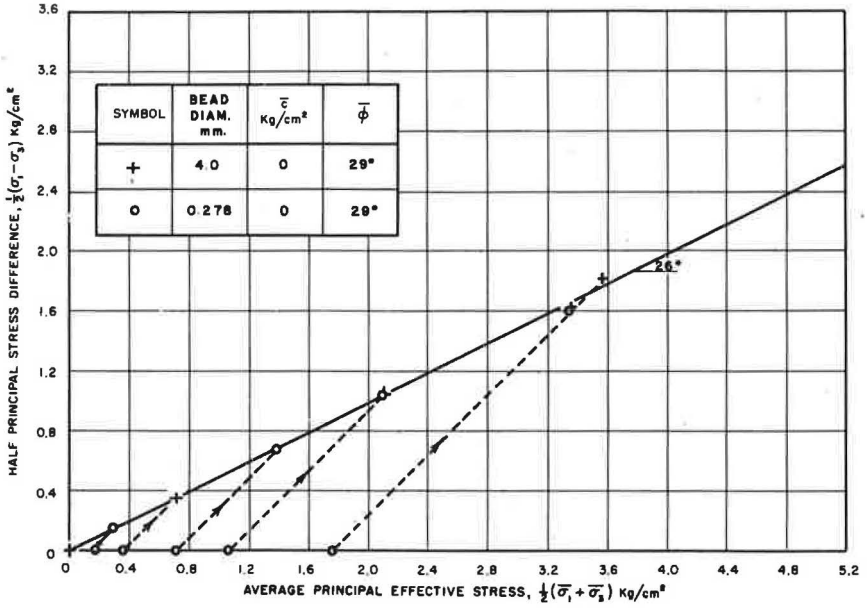

Figure 9. Influence of bead size on the effective stress-strength behavior of plain bead systems sheared at 0.1 percent axial strain per min.

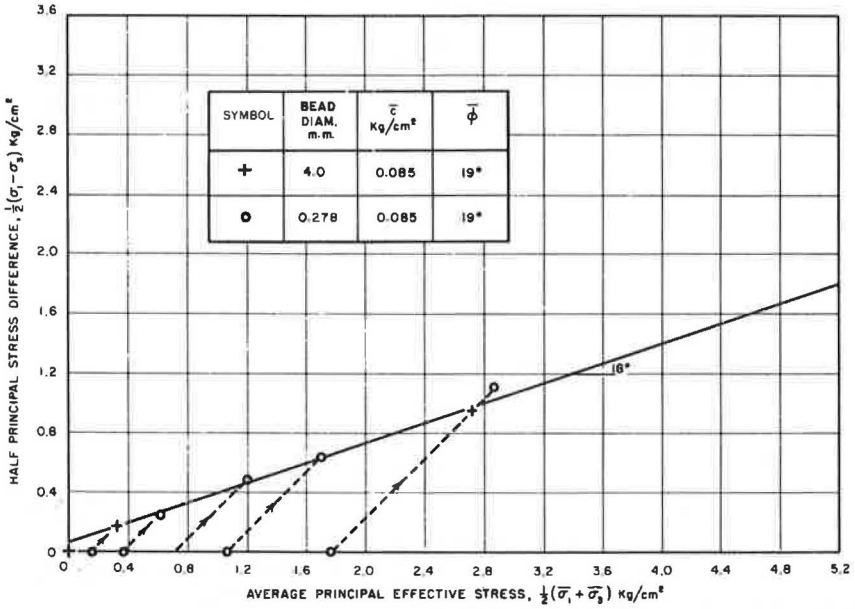

Figure 10. Influence of bead size on the effective stress-strength behavior of asphalt-bead systems sheared at 0.1 percent axial strain.

9 percent asphalt is shown in Figure 8 as a function of consolidation pressure and axial strain. Above 1 percent axial strain the high-density samples exhibited dilatancy over the full range of consolidation pressures investigated. The dilatancy increased with increasing axial strain and with decreasing consolidation pressure. The low-density

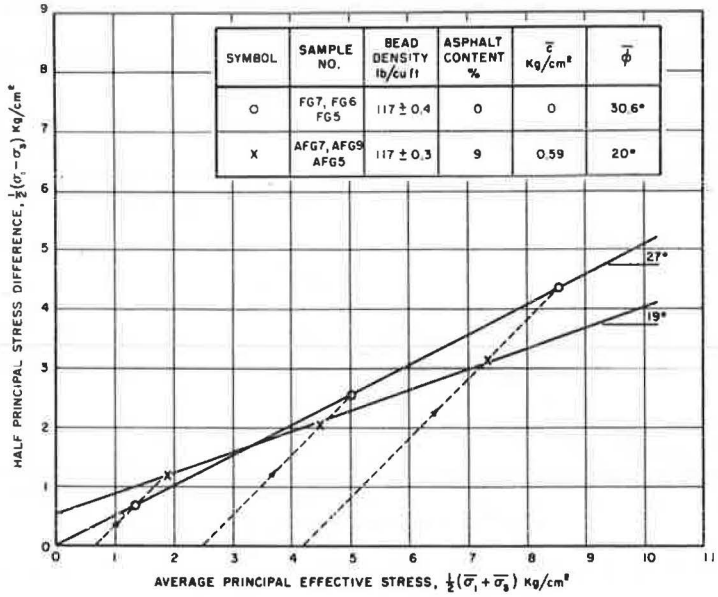

Figure 11. Influence of asphalt on the effective stress-strength behavior of well-graded beads.

samples at all consolidation pressures above 0.8 kg/cm^2 showed a volume decrease during drained shear that increased with increasing consolidation pressure and increasing axial strain. At all axial strains the differences in volume change between the high- and low-density specimen was essentially independent of consolidation pressure. The overall volume-change behavior of the glass beads with asphalt is similar to that observed with plain sands.

Influence of Bead Size—A change in the maximum particle size of a cohesionless particulate system should not alter its effective stress-strength behavior provided the particle size distribution, the particle shape, and the density of samples are kept constant. This was verified by conducting consolidated-drained triaxial compression tests at five different consolidation pressures on samples prepared with 0.278-mm and 4.0-mm diameter glass spheres compacted to 90.1 ± 1.9 lb/cu ft. The results of these tests are given in Figure 9, which shows that the Mohr-Coulomb effective stress envelope is independent of particle size per se. Both bead sizes had an effective angle of internal friction of 29° and zero effective cohesion intercept.

In order to check that this was also true for samples containing asphalt, test specimens were prepared using the 4-mm and 0.278-mm beads and 9 percent asphalt by weight, with the same bead density as the untreated samples. These samples were tested in exactly the same way as the beads without asphalt. The testing temperature was closely controlled at 21 ± 0.5 C, and samples were sheared at 0.1 percent axial strain per min. Here again the bead size had no effect on the Mohr-Coulomb effective stress-strength envelope (Fig. 10). It can be seen from Figures 9 and 10 that the addition of asphalt caused a reduction in the effective angle of internal friction of 10° and made the systems exhibit a small effective cohesion intercept of 0.08 kg/cm^2. Additional results showing the effect of asphalt on the shear strength behavior of various aggregate systems are given in other sections of this report.

Influence of Bead Gradation—In order to investigate the effects of bead gradation on the strength and volume change behavior, a well-graded aggregate consisting of spherical beads was tested with and without asphalt in drained triaxial shear. Tests were run at 1 percent axial strain per minute, 20 C, and over a range of effective confining pressures from 0.703 kg/cm^2 to 4.22 kg/cm^2. The aggregate consisted of the graded bead system described earlier at a density of 117 lb/cu ft.

The strength envelopes obtained from these tests are shown in Figure 11. As in the case of the single-size 0.278-mm glass beads, there was no cohesion intercept, $\bar{c}$, for the samples without asphalt. The friction angle of 30.6° was lower than the 39° obtained with the plain 0.278-mm beads. With all other conditions equal, a well-graded sand will have a higher friction angle than a uniform sand. The lower angle of friction is probably due to the well-graded beads having a lower relative density. This could be seen from the fact that they exhibited less dilation during shear than the corresponding uniform bead samples.

As was the case with the plain uniform bead system, the addition of asphalt caused a friction angle drop (from 30.6° to 20°) and a cohesion intercept (0.59 kg/cm^2). This would again indicate that the asphalt acts as a lubricant.

Figure 12 shows typical stress-strain and volume-change curves for the well-graded beads with and without asphalt. The stress-strain curves for the plain beads rose sharply until failure. This was immediately followed by sharp fluctuations indicating stick-and-slip friction behavior throughout the remainder of the test. It was noticed that the amplitude of the fluctuations increased with increasing effective confining pressure, while the frequency decreased. According to Bowden, Leben, and Tabor (2), stick-slip sometimes occurs when unlubricated, like materials slide upon one another.

The stress-strain curves for the 9 percent asphalt system were much the same as the corresponding curves for the 0.278-mm beads and asphalt. They did not exhibit the stick-slip behavior observed with the plain beads because of the lubricating influence of the asphalt.

The volume-change curves showed an initial negative volume change as experienced in the previous tests. The volume-strain curves show dilation in all tests decreasing with increasing effective confining pressure.

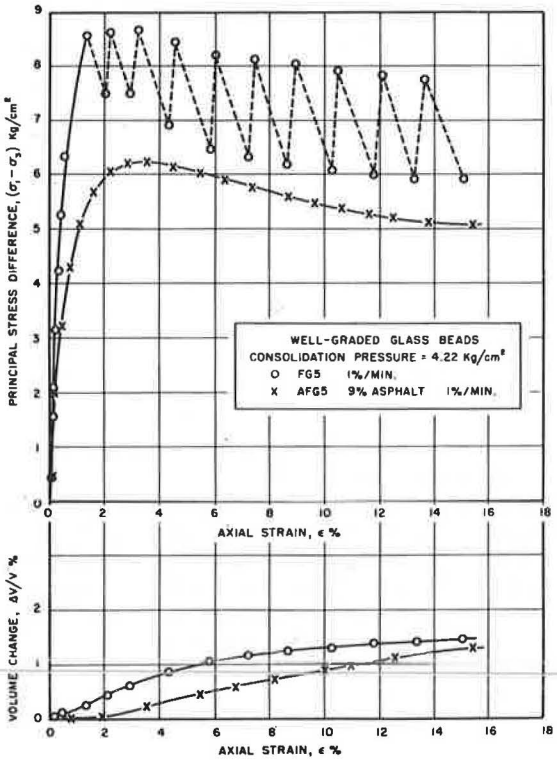

Figure 12. Influence of asphalt on the stress-strain and volume change behavior of well-graded glass beads.

The volume change vs consolidation pressure curves of Figure 13 show a much greater decrease in volume change with increasing consolidation pressure for the bead-asphalt system than for the plain beads. The uniform bead systems exhibited a similar behavior, as was discussed earlier.

Additional tests were run with and without asphalt on the same bead gradation but at lower bead densities. The plain beads were at a density of 107 lb/cu ft and the asphalt-bead samples at 110.5 lb/cu ft bead density. The strength envelopes, along with those of the higher-density systems, are shown in Figure 14.

A reduction of 10 lb/cu ft in the density of the plain bead samples caused the friction angle to drop from 30.6° to 21.3°. A drop of 6 lb/cu ft in the density of the asphalt-bead samples caused no decrease in the friction angle. Thus, while a decrease in density caused a considerable drop in friction angle for the plain bead system, no change in friction angle with density occurred with the asphalt-bead system. This is consistent with the observations made on the 0.278-mm bead-asphalt system.

Decreasing the density was found to decrease the cohesion from 0.59 to 0.21 kg/cm^2. On the 0.278-mm bead-asphalt system no significant change in cohesion with density was noticed. This seems to present an inconsistency. If cohesion is due to the asphalt at the bead-to-bead contacts, an increase in density increases the number of contacts and therefore should increase the cohesion. An increase in density of the samples with the one-size aggregate did not significantly increase the number of bead-to-bead contacts and therefore did not increase the cohesion. With a well-graded system the number of contacts can increase substantially with increasing density, since the number of particles per unit volume is considerably larger than that for a uniform aggregate and therefore the cohesion should be more sensitive to change in density.

Sand-Asphalt System—A test program identical to the preceding was carried out on a well-graded Ottawa sand with ground flint powder fines. Tests were run on two series of samples, one without asphalt and the other with 9 percent asphalt by weight. All samples were at 129.8 lb/cu ft aggregate density. Both series were tested at consolidation pressures ranging from 0.703 to 4.22 kg/cm^2 at a temperature of 20 C and a strain rate of 1 percent per min. The plain samples failed along a single inclined failure surface while the asphalt samples failed by bulging.

The Mohr-Coulomb strength envelopes are shown in Figure 15. As is common for a dense sand, the envelope is slightly curved with no cohesion and a friction angle dropping from an initial 54° to 41.5°. This steep envelope compares to a $\bar{\phi}$ of only 30.6° for the well-graded glass beads. Two factors influence this increase: first, the material is quartz, which has different frictional properties than the crown-barium glass, and, second, the sand and ground flint grains are not perfectly spherical, resulting in more interlocking and less rolling during shear.

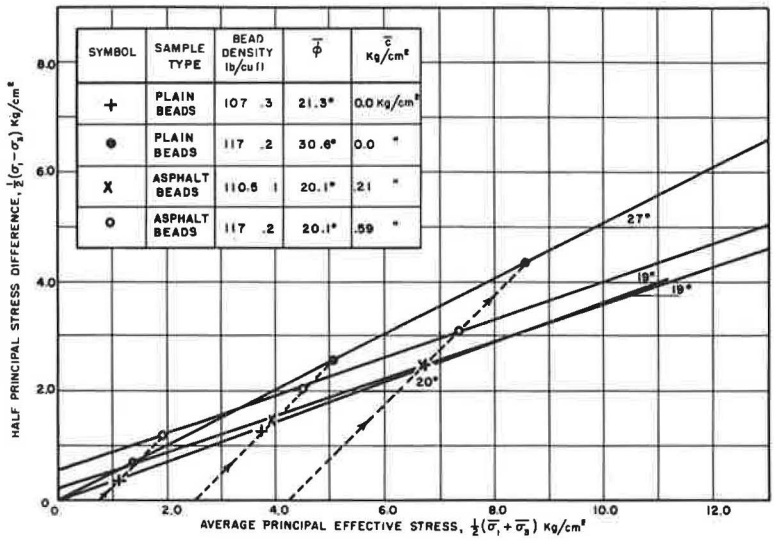

Figure 13. Influence of asphalt on the dilation of well-graded glass beads.

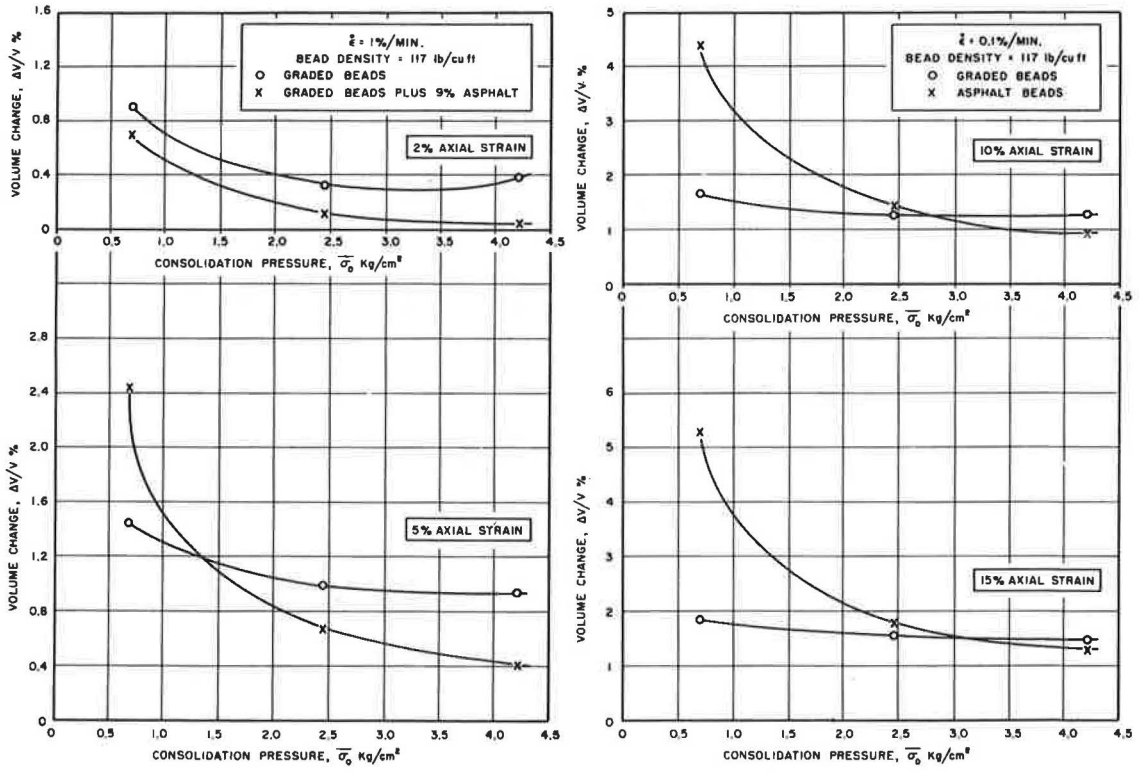

Figure 14. Influence of bead density on the effective stress-strength behavior of well-graded beads.

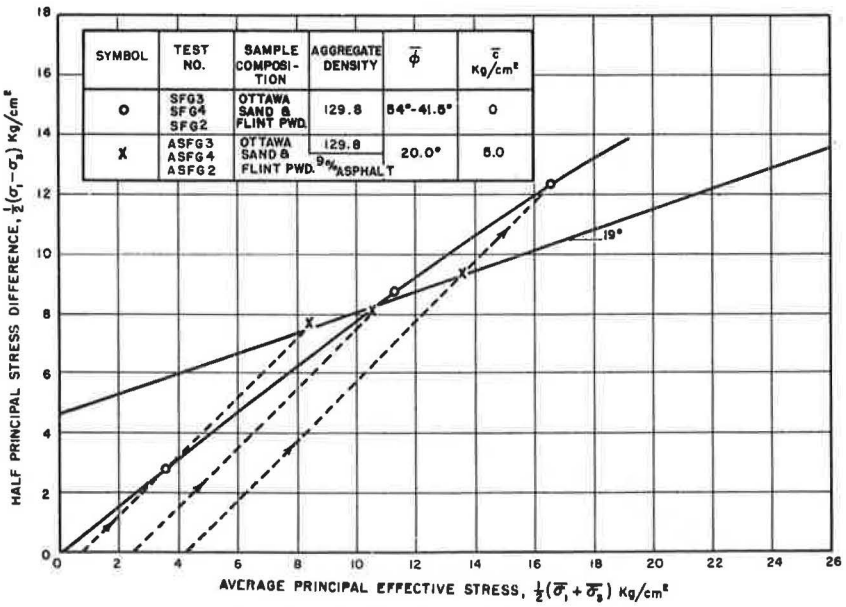

Figure 15. Influence of asphalt on the effective stress-strength behavior of well-graded Ottawa sand and flint powder.

For the sand-asphalt system, the friction angle of 20° is the same as that for the well-graded bead-asphalt system. Since the asphalt acts as a lubricant, it seems that the material it lubricates does not affect the friction angle. The degree of angularity introduced by the Ottawa sand and flint powder apparently was not sufficient to affect the friction angle when the material was lubricated by an asphalt film.

The cohesion intercept of 5.0 kg/cm^2 due to the addition of the asphalt is very large compared with the 0.59 kg/cm^2 obtained with the addition of asphalt to the well-graded bead system. The air void space of these samples was only about 2.5 percent of the total volume (compared with 9 percent for the well-graded beads with asphalt), indicating that the samples were nearly saturated with asphalt. This in turn means that this system had many more particle-to-particle contacts than the well-graded bead system, which explains the higher cohesive resistance.

Environmental Factors

Influence of Strain Rate—Consolidated-drained triaxial compression tests were run on 0.278-mm glass bead samples with 9 percent asphalt (97.0 lb/cu ft average density of beads) at three axial strain rates, 0.1, 1.0 and 10.0 percent per min. The tests were run over a range of consolidation pressures from 0.141 to 2.42 kg/cm^2 at a temperature of 21 C. All samples exhibited a bulging mode of failure. The strength envelopes for the three rates of strain are shown in Figure 16.

Over the range of strain rates investigated there was no significant change in the friction angle. There seemed to be a slight trend toward a decrease in friction angle with increasing strain rate, but this was only 2½° over a hundredfold increase in rate. Such a small change is well within the range of experimental error and cannot be considered significant. Unfortunately, higher strain rates could not be achieved with the equipment used in this investigation.

The cohesion increased rapidly with increasing strain rate. Figure 17 is a plot of the effective cohesion intercept vs rate of axial strain plotted on log-log paper. It is well within the experimental error to consider these points to lie on a straight line defined by the equation

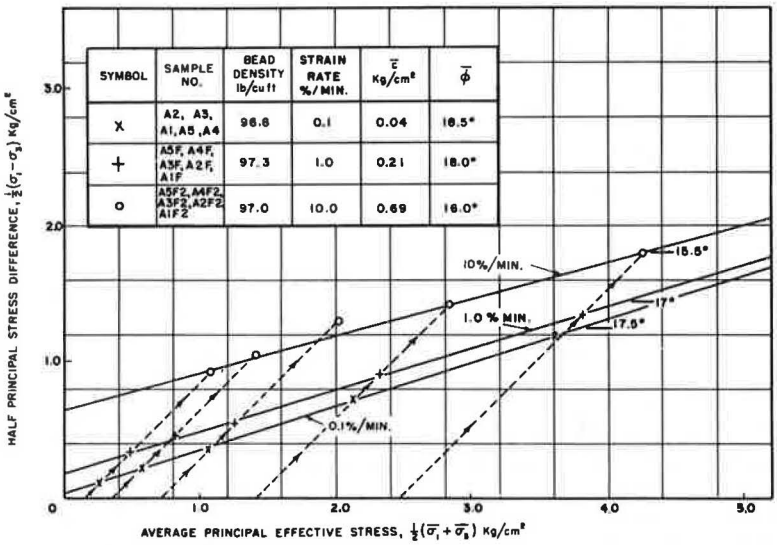

Figure 16. Influence of strain rate on the effective stress-strength behavior of 0.278-mm beads plus 9 percent asphalt.

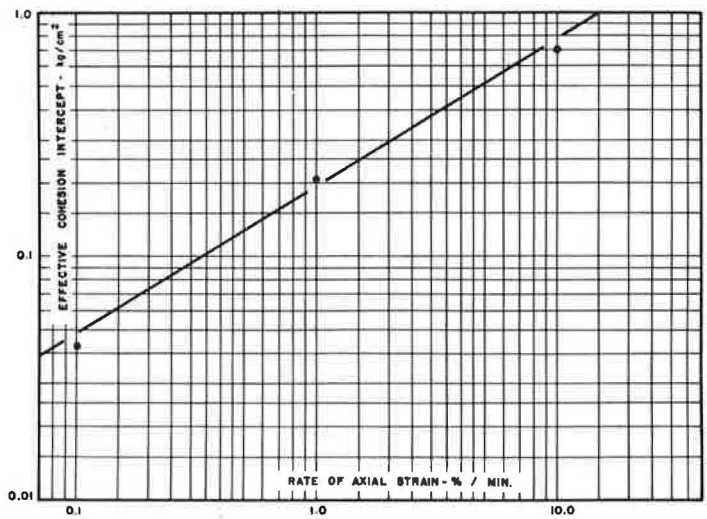

Figure 17. Influence of rate of strain on the effective cohesion intercept of 0.278-mm beads plus 9 percent asphalt.

$$\log_{10} \bar{c} = \log_{10} 0.192 + 0.62 \log_{10} \dot{\epsilon}$$

which can be rewritten as

$$\bar{c} = 0.192 \, (\dot{\epsilon})^{0.62}$$

where $\bar{c}$ is the effective cohesion intercept in kg/cm^2 and $\dot{\epsilon}$ is the axial strain rate in percent per minute. The constants of this equation obviously apply only for the 0.278-mm

bead system with 9 percent asphalt at 21 C. The influence of strain rate on the strength behavior of this system can therefore be represented by

$$\tau_{ff} = 0.192\ (\dot{\epsilon})^{0.62}\ \text{kg/cm}^2 + \bar{\sigma}_{ff} \tan 17.5^\circ$$

The effect of strain on the other systems has not been investigated; however, it is reasonable to assume that a similar relationship would exist, given by an equation of the following form:

$$\tau_{ff} = A(\dot{\epsilon})^B\ \text{kg/cm}^2 + \bar{\sigma}_{ff} \tan \bar{\phi}$$

where A and B are constants to be determined experimentally and $\bar{\phi}$ is the effective angle of internal friction obtained from consolidated drained triaxial tests at a single strain rate.

It is interesting to note that, assuming the above equation holds for all asphalt systems, theoretically only two tests at the same consolidation pressure but at different strain rates are needed to determine the constants A and B.

Typical stress-strain and volume change curves are shown in Figure 18. For low rates of axial strain, the stress-strain curves rose sharply to a peak and then leveled off at a nearly constant value. For the higher strain rates, the curves peaked and then dropped, tending to level off after dropping. The higher the strain rate, the more pronounced was the hump at the peak stress.

Krokosky (8) showed the asphalt used in road materials to be an ideal linear viscoelastic material. As such it is capable of both energy storage and dissipation. The difference in the stress-strain curves is believed due to strain energy stored and released by the sample during the tests. At the higher strain rates a greater amount of strain energy is stored in the samples than at the lower rate. The humps in the stress-strain curves are due to large amounts of strain energy being stored and then released as the samples fail. At large strains, when the shearing resistance of the specimens reaches a constant value, the rate of storage becomes equal to the rate of dissipation of energy. Since the angle of internal friction of the asphalt-bead system was independent of rate of strain, the cohesion intercept should have represented the same rate of strain properties as the asphalt binder, i.e., $\bar{c}$ should have increased linearly with increasing rate of strain. It is evident from the results presented that this was not the case. A partial explanation can be obtained by examining the volume change behavior as a function of rate of strain.

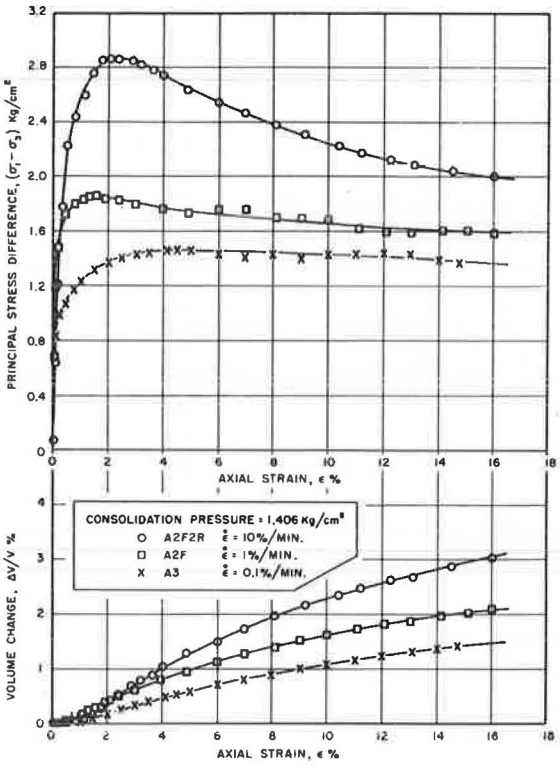

Figure 18. Influence of strain rate on the stress-strain and volume change behavior of 0.278-mm beads plus 9 percent asphalt.

Figure 19 shows that rate of strain influences the magnitude of the volume change during shear. At a given consolidation pressure and axial strain, the faster the rate of strain, the larger the observed dilation. This means that failure occurred more

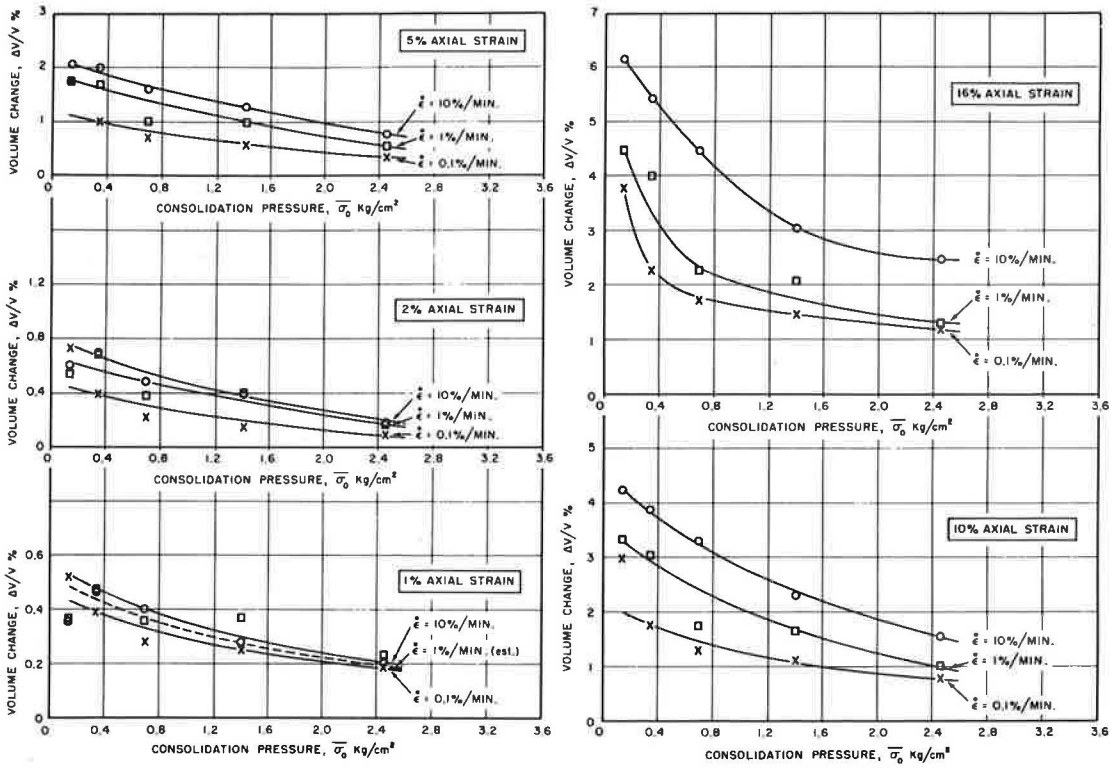

Figure 19. Influence of strain rate on the dilation of 0.278-mm beads plus 9 percent asphalt.

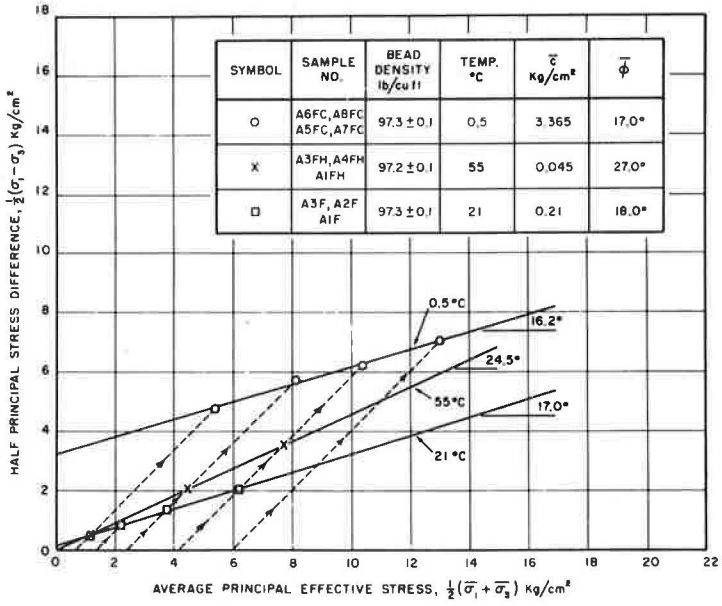

Figure 20. Influence of temperature on the effective stress-strength behavior of 0.278-mm beads plus 9 percent asphalt.

easily at the lower rates of strain. A similar phenomenon has been observed with untreated sands (5). At low rates of strain, particles have more time to relocate during shear and therefore cause less interference along the potential failure surfaces. As the rate of strain increases, the viscous nature of asphalt makes it more difficult for particles within the potential failure zone to relocate and thus the failure becomes less efficient and involves larger dilation of the specimens. In addition, at the faster strain rates there is less time for progressive relocation of particles in the failure zone. The combination of these effects can contribute to the nonlinear viscoelastic behavior of asphaltic concrete. The observed rate of increase in cohesion with increasing rate of strain was less than would be observed for linear viscoelastic material. This could be due to fewer particles moving relative to each other at the faster strain rates, since the failure is less efficient and the failure zone less extensive.

Influence of Temperature—In order to study the influence of temperature per se on the strength behavior of asphalt-bead systems, three sets of tests were conducted at 0.5, 21, and 55 C. The samples for the three sets of tests were prepared with the 0.278-mm beads and 9 percent asphalt. The specimens were then consolidated, saturated, and tested in drained shear at the above temperatures. A rate of axial strain of 1 percent per min was used for all these tests. The Mohr-Coulomb strength envelopes at 0.5, 21, and 55 C are shown in Figure 20.

Lowering the temperature from 21 to 0.5 C had no significant effect on the friction angle, but raising the temperature from 21 to 55 C caused a very significant increase in the friction angle, from 18.0° to 27.0°. On the other hand, lowering the temperature caused a large increase in the cohesion but raising the temperature caused it to drop only slightly.

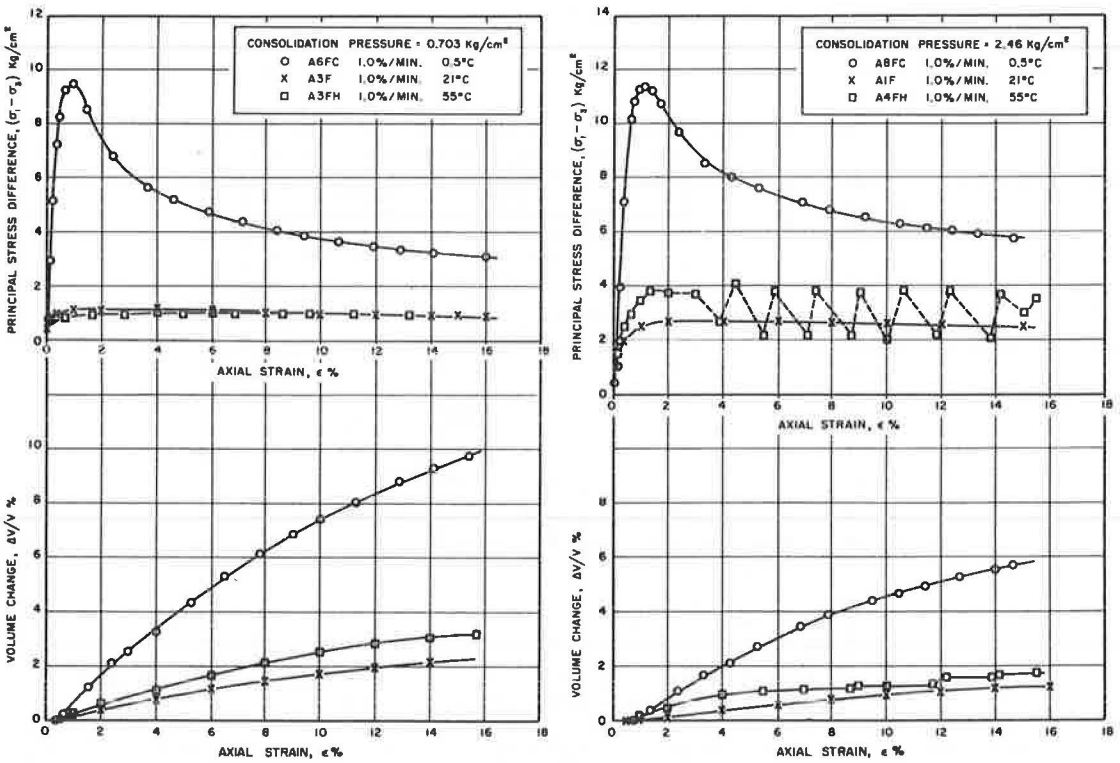

Figure 21. Influence of temperature on the stress-strain and volume change behavior of 0.278-mm beads plus 9 percent asphalt.

Nijboer (11) reported similar results but did not note any increase in friction angle at higher temperatures. However, the highest temperature used in his investigation was only 40 C. Nijboer showed that at some temperature below 20 C the value of the cohesion begins a rapid increase. Likewise, for this bead-asphalt system, it is believed that at some temperature above 21 C the angle of friction starts increasing toward that of the plain aggregate system.

The rise in cohesion at low temperatures seems to be analogous to the rise in cohesion with increasing rate of axial strain. Both factors have the same general effect on the shearing resistance of the asphalt binder.

The rise in the friction angle at high temperatures seems to be caused by a partial breakdown in the asphalt film at points of contact between particles moving relative to one another. This is due to the lower strength of the asphalt film at high temperatures, which results in some glass to glass contact. At 55 C the angle of friction had increased from 17 to 27°. Obviously, at this temperature only partial breakdown of the asphalt films had occurred, since the angle of friction was still less than the 34° observed for the plain uniform beads.

The stress-strain and volume change curves are shown in Figure 21. The curves at 21 C rose sharply and then flattened to a nearly constant stress level throughout the remainder of the tests. Those at 0.5 C rose sharply to a high peak and then dropped off considerably on further straining. Those at 55 C and the higher consolidation pressures rose steeply, bent over, and then started a series of violent fluctuations throughout the remainder of the tests.

The stress-strain curves for the 0.5 C tests have peaks similar to those run at the high strain rate shown earlier. Similarly, these peaks are caused by the samples absorbing and releasing strain energy.

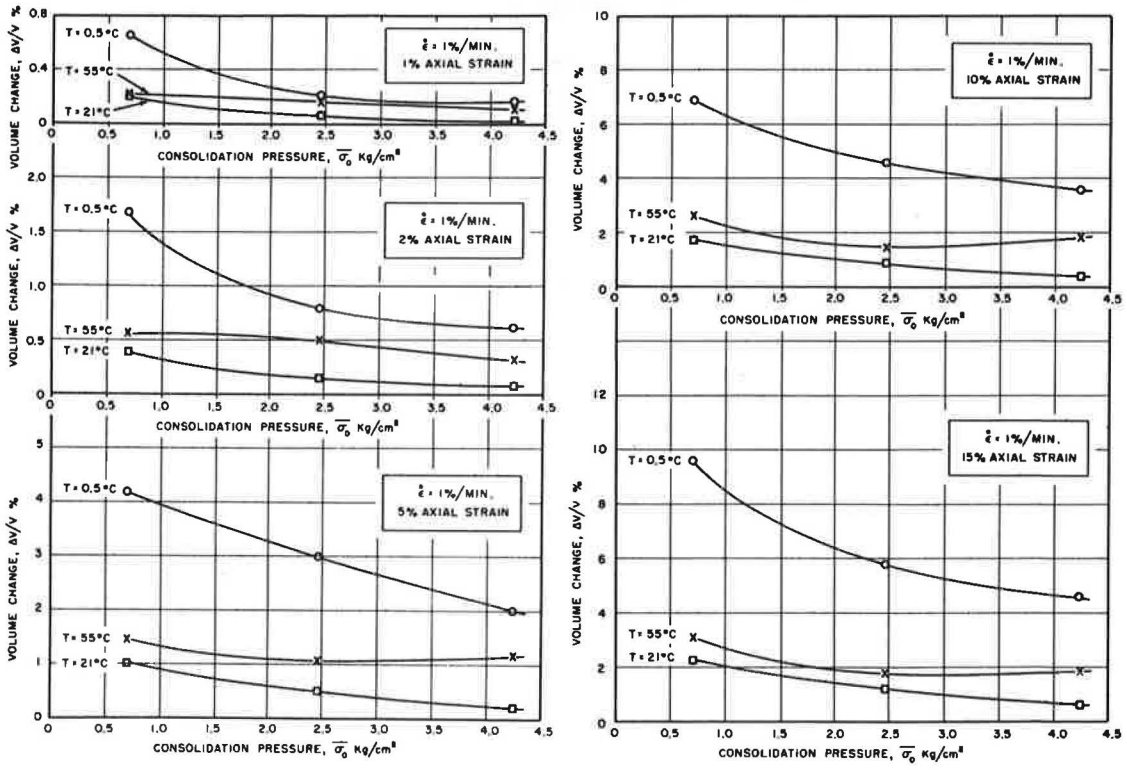

Figure 22. Influence of temperature on the dilation of 0.278-mm beads plus 9 percent asphalt.

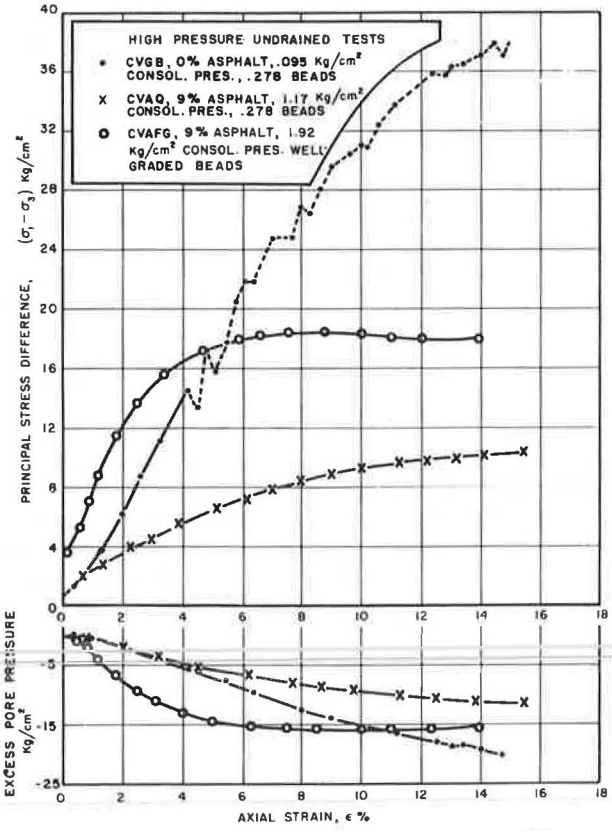

Figure 23. Stress-strain and pore pressure response curves for undrained tests on various bead systems.

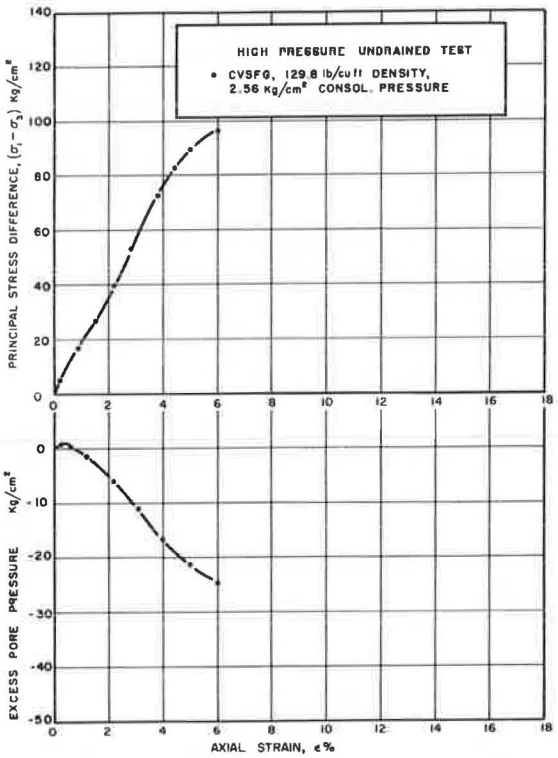

Figure 24. Stress-strain and pore pressure response curves for undrained test on well-graded Ottawa sand and flint powder.

The violent fluctuations in the stress-strain curves of the high-temperature tests are caused by stick-and-slip friction phenomena due to a partial tearing of the lubricating asphalt film (13). This supports the explanation that the increase in friction angle is caused by a breakdown in the lubrication qualities of the asphalt, allowing some mineral-to-mineral contact of the aggregate and the subsequent increase in friction angle.

The 55 C test at the low effective confining pressure showed no signs of stick-slip behavior. This indicates that either the magnitude of the fluctuations was too small to measure with the equipment or that no stick-slip was taking place. If the latter is the case, then evidently the effective confining pressure was not large enough to cause stick-slip even though a breakdown in the asphalt film between particles occurred. Stick-and-slip would then have a minimum normal stress below which it does not occur.

The low-temperature tests showed by far the greatest volume dilations during shear (Fig. 22). The situation is analogous to that of the samples at the high rate of axial shear explained in the preceding section. Instead of high strain rate lowering the failure of efficiency, the high viscosity of the asphalt at the low temperatures and the poor lubrication qualities of the asphalt at the high temperatures tend to lower the efficiency.

Influence of Volume Change—In order to study the influence of restricting volume changes during shear on the strength behavior of the various systems, duplicates of some of the different samples used were tested at constant volume (consolidated-undrained shear). This was achieved by consolidating and saturating the triaxial test specimen under a back pressure of approximately 67 kg/cm^2 and cell pressure of about 68 kg/cm^2, giving an effective consolidation pressure of approximately 1 kg/cm^2. The pore water lines were then closed off and the samples sheared at 1 percent axial strain per min and 21 C. By closing off the pore water lines the volume of the specimens was maintained constant during shear. During shear the cell pressure was kept constant and pore water pressure change was measured by means of a transducer.

The stress-strain and pore pressure behavior in undrained shear of the plain uniform bead system and the plain well-graded sand system are shown in Figures 23 and 24. It can be seen that the shearing resistance of the specimens kept increasing while the

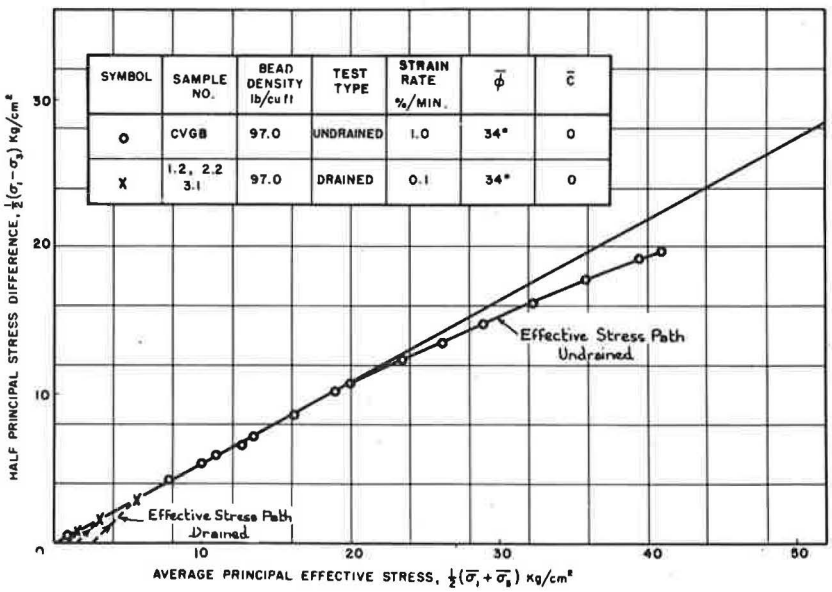

Figure 25. Effective stress-strength behavior of 0.278-mm glass beads in drained and undrained compression.

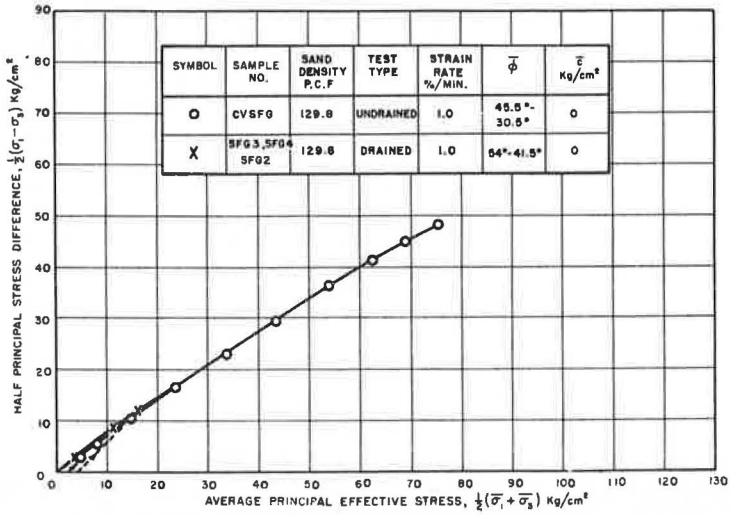

Figure 26. Effective stress-strength behavior of well-graded Ottawa sand and flint powder in drained and undrained compression.

excess pore pressures kept becoming more negative with increasing axial strain. The tendency for the specimens to dilate during shear caused the drop in excess pore pressure, which in turn increased the average effective stress within the sample. The increase in average effective stress increased the shearing resistance by increasing the normal effective stress on the failure planes.

Figures 25 and 26 show the effective stress paths of the plain uniform bead system and the graded sand system in undrained shear. Also included in these figures are the

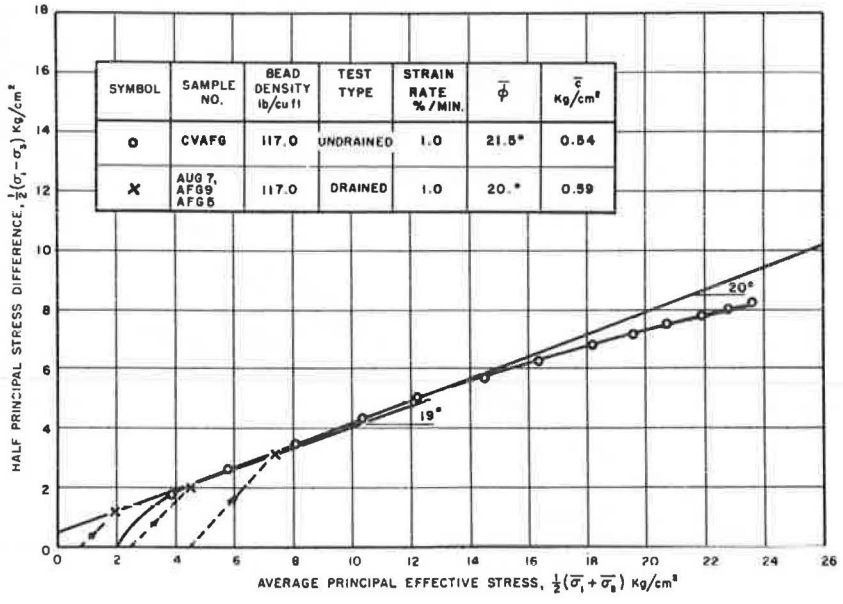

Figure 27. Effective stress-strength behavior of well-graded beads plus 9 percent asphalt in drained and undrained compression.

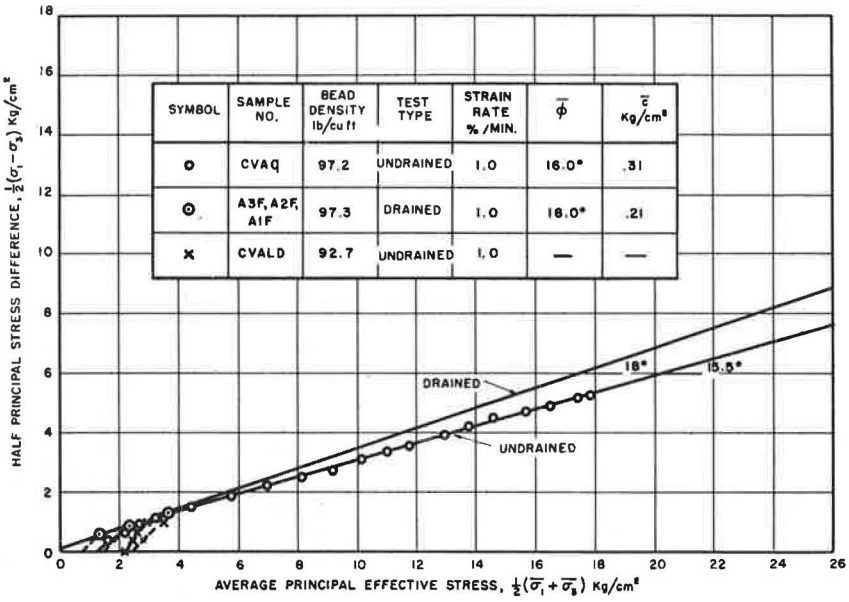

Figure 28. Effective stress-strength behavior of 0.278-mm beads plus 9 percent asphalt in drained and undrained compression.

effective stress envelopes for the corresponding drained tests. The effective stress paths of the undrained tests became essentially tangent to the drained envelopes at relatively low shear stresses and then followed the envelopes for some distance before dropping off. This means the drained and undrained tests on the untreated systems give essentially the same envelope even though the undrained tests have considerably higher strength. The higher strengths are due to the increase in average effective stress resulting from the negative excess pore pressures developed during shear. In drained tests the pore pressures during shear remain constant at their initial value and therefore have no influence on the measured strengths.

In the preceding section it was observed that for stick-slip behavior to occur during shear a minimum normal effective stress was possibly needed. From Figure 23 it can be seen that, in the case of the uniform plain beads, stick-slip behavior only started at approximately 4 percent axial strain, which corresponded to an average effective stress of about 13 kg/cm^2. This suggests that there is a threshold effective stress below which stick-slip does not occur, even when the system does not contain asphalt. This threshold is also probably a function of the particle size gradation and dry density of the system.

Figures 27 and 28 show the influence of drainage conditions during shear on the effective stress-strength behavior of some of the asphalt systems. It can be seen from Figure 27 that the effective stress-strength parameters, $\bar{\phi}$ and $\bar{c}$, of the well-graded beads with 9 percent asphalt are essentially the same in drained and undrained shear. However, due to the negative excess pore water pressures, which developed during undrained shear (see Fig. 23), the undrained samples were at least four times stronger than the corresponding drained samples consolidated at the same pressure. This behavior is similar to that observed with the plain systems, i.e., the effective stresses rather than the total stresses also control the strength behavior of asphaltic concrete.

The influence of bead density on the stress-strain and excess pore water pressure behavior of the uniform beads with 9 percent asphalt is shown in Figure 29. The high-density sample developed large negative excess pore pressures during shear, whereas the low-density sample started out developing a small positive excess pore pressure, which became slightly negative at large strains. The difference in pore pressure be-

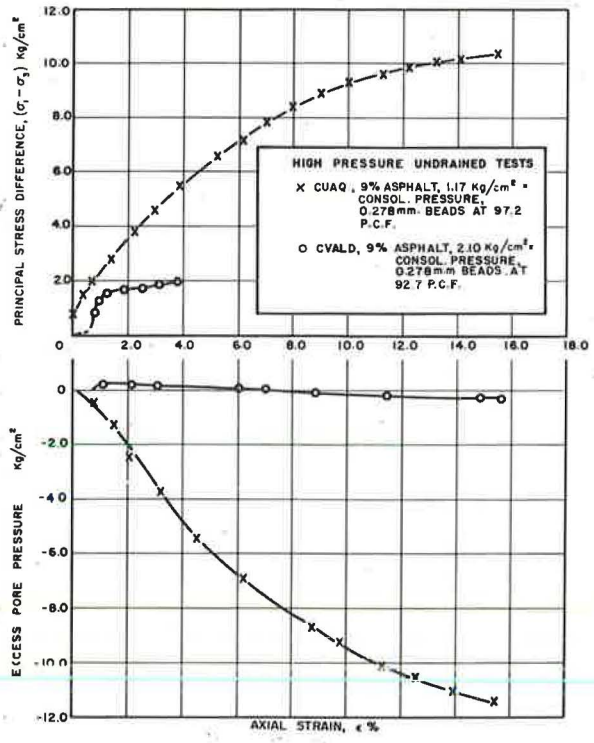

Figure 29. Stress-strain and pore pressure response curves for undrained tests on high- and low-density uniform beads plus asphalt.

havior of the low- and high-density samples caused the high-density sample to be over five times stronger than the low-density sample. In terms of effective stresses, both samples shared essentially the same strength envelope (Fig. 28).

It is evident from the experimental results that the magnitude of the volume changes during shear can appreciably influence the maximum shear strength of asphaltic concrete. In general, asphaltic concrete contains air voids that are compressible and will allow some change in volume of the concrete during shear. Since the asphalt and aggregate are relatively incompressible, the volume change during shear will be a function of the amount of air in the system. As the air content in the concrete increases, the resistance to volume changes during shear decreases and consequently the strength decreases for a given aggregate density. In practice, it is not possible to eliminate all air voids by increasing the asphalt content without decreasing the aggregate density and therefore reducing the beneficial interlocking influence of the aggregate on the strength. Furthermore, complete elimination of air voids can result in a reduction of the residual negative fluid pressure in the asphalt after compaction. This would cause a decrease in the residual effective stress (consolidation pressure) in the concrete after compaction and therefore a decrease in its strength. It follows that for practical reasons a small percentage of air voids should exist in compacted asphaltic concrete and consequently some volume change will occur during shear. For maximum strength, this volume change should be kept to a minimum by reducing as far as possible the percentages of air voids without reducing the aggregate density or the residual effective stress after compaction.

SUMMARY, CONCLUSIONS, RECOMMENDATIONS

The strength behavior of bituminous concrete was investigated using both drained and undrained triaxial compression tests to determine the basic Mohr-Coulomb strength parameters, effective angle of internal friction, and effective cohesion of various aggregate and asphalt-aggregate systems, and the influence of the stress-strain, volume-change, and excess pore pressure behavior on these parameters.

The systems investigated were selected so as to isolate and determine the influence of the more important individual compositional factors on the strength behavior of asphaltic concrete. These included asphalt content, aggregate grain size, aggregate density, aggregate gradation, and aggregate material and grain shape. In addition, environmental factors of strain rate, temperature, and volume change were studied.

Using a uniform spherical sand-sized aggregate of glass beads, it was found from drained triaxial compression tests that

1. The introduction of asphalt produced an effective cohesion and a considerable drop in the effective angle of internal friction, and
2. Neither this angle of internal friction nor the resultant effective cohesion was significantly affected by changes in aggregate grain size, asphalt content, or aggregate density.

Using a well-graded glass bead aggregate in drained triaxial compression, it was found that

1. The introduction of asphalt again produced an effective cohesion and a drop in angle of internal friction, and
2. The effective angle of internal friction was also independent of aggregate density, but in this case the effective cohesion decreased with a decrease in density.

A similar reduction in effective angle of internal friction was observed on the addition of asphalt to a well-graded sand. With this system the asphalt produced a considerably larger effective cohesion than had been observed with the glass bead systems.

Environmental factors of strain rate and temperature were studied on the strength behavior of the uniform bead-asphalt system in drained triaxial compression. It was found that

1. The effective angle of internal friction was independent of rate of axial strain while the effective cohesion increased with increasing strain rate, and
2. High temperatures caused an increase in the effective angle of internal friction with little change in effective cohesion, whereas low temperatures resulted in a large increase in effective cohesion with no significant change in internal friction angle.

Undrained triaxial compression tests were conducted on some of the systems that had been studied in drained triaxial shear. In all cases, there was no significant change in either the effective angle of internal friction or the effective cohesion. The undrained shear strength of all samples with a high-aggregate density was much larger than the corresponding strengths obtained in the drained tests. Drainage conditions did not significantly influence the strength of the low-aggregate density systems.

The influence of the compositional and environmental factors on the effective stress-strength parameters of the systems studied in this investigation is summarized in Table 1.

From the results of the experimental investigation it can be concluded that

1. The effective stresses rather than the total stresses control the strength behavior of asphaltic concrete.
2. The addition of asphalt to a cohesionless aggregate system will cause it to exhibit an effective cohesion intercept at failure due to the viscous nature of asphalt. However, its effective angle of internal friction (as determined from the Mohr-Coulomb criterion of failure) is considerably reduced due to the lubricating effect of the asphalt.
3. The effective cohesion is a function of strain energy stored in the asphalt binder during shear. The energy storage capacity, and therefore effective cohesion, increases with increasing strain rate, decreasing temperature, and increasing amount of asphalt undergoing strain.
4. The effective friction angle increases only when the lubrication qualities of the asphalt decrease, due to either high temperatures or very low asphalt contents.
5. Restricting sample volume change during shear has no effect on the Mohr-Coulomb effective stress-strength parameters, but can result in a large increase in strength if the sample has a tendency to dilate during shear.
6. The volume change behavior during drained shear not only is a function of the compositional factors such as density, gradation, and angularity of the aggregate and the asphalt type and content, but also depends on the environmental factors such as temperature and rate of strain.

Practical Implications

Some practical implications resulting from this investigation can be summarized as follows:

TABLE 1

SUMMARY OF MOHR-COULOMB PARAMETERS

Sample Composition	Aggregate Dry Density (lb/cu ft)	Strain Rate (%/min)	Temperature C	$\bar{\phi}$ (degrees)	$\bar{C}$ (kg/cm^2)	Drainage Conditions
Uniform 0.278-mm beads	97.0	0.1	21	34	0.0	Drained
Uniform 0.278-mm beads plus 9 percent asphalt	96.8	0.1	21	18.5	0.042	Drained
Uniform 0.278-mm beads plus 9 percent asphalt	97.3	1.0	21	18.0	0.21	Drained
Uniform 0.278-mm beads plus 9 percent asphalt	97	10.0	21	16.0	0.69	Drained
Uniform 0.278-mm beads plus 9 percent asphalt	92.7	1.0	21	16	0.16	Drained
Uniform 0.278-mm beads plus 9 percent asphalt	99.2	1.0	21	17.5	0.23	Drained
Uniform 0.278-mm beads plus 6 percent asphalt	97.2	1.0	21	15.5	0.23	Drained
Uniform 0.278-mm beads plus 3 percent asphalt	97.3	1.0	21	15.5	0.18	Drained
Uniform 0.278-mm beads plus 9 percent asphalt	97	1.0	55	27.0	0.045	Drained
Uniform 0.278-mm beads plus 9 percent asphalt	97	1.0	0.5	16.9	3.37	Drained
Well-graded beads	107	1.0	21	21.3	0.0	Drained
Well-graded beads	117	1.0	21	30.6	0.0	Drained
Well-graded beads plus 9 percent asphalt	110.5	1.0	21	20.1	0.21	Drained
Well-graded beads plus 9 percent asphalt	117	1.0	21	20.1	0.59	Drained
Well-graded Ottawa sand and flint powder	129.8	1.0	21	54-41.5	0.34	Drained
Graded Ottawa sand and flint powder plus 9 percent asphalt	129.8	1.0	21	20.0	5.0	Drained
Uniform 0.278-mm beads	97	1.0	21	34	0.0	Undrained
Uniform 0.278-mm beads plus 9 percent asphalt	97.2	1.0	21	16	0.31	Undrained
Uniform 0.278 mm beads plus 9 percent asphalt	92.7	1.0	21	—	—	Undrained
Well-graded beads plus 9 percent asphalt	117	1.0	21	21.5	0.54	Undrained
Well-graded Ottawa sand and flint powder	129.8	1.0	21	45.5-30.5	0	Undrained

1. Optimum compaction of asphaltic concrete should occur when the shearing resistance of the mix during compaction is a minimum. At a given rate of strain, the effective cohesive resistance decreases with increasing temperature, whereas the effective frictional resistance decreases with decreasing temperature. Therefore, optimum compaction should occur at a temperature where the sum of the frictional and cohesive resistances is a minimum.
2. Increasing the compaction effort can result in an increase in the shear strength of asphaltic concrete, provided it decreases the air void content and increases the aggregate density without causing a significant reduction in the residual negative fluid pressure in the asphalt.
3. For a given asphaltic concrete, the magnitude of the volumetric strain during shear is dependent on the rate of strain and the temperature. Any theoretical model for asphaltic concrete should therefore take these effects into consideration.

Recommendations

Due to time limitations, it was not possible to carry out this investigation to completion. The influence of asphalt on the coefficient of sliding friction of the glass beads and the sand grains should be determined. This would involve conducting direct shear tests on these aggregates sliding over a smooth surface of the same material in order to eliminate the effects of interlocking.

To generalize the findings reported here, angular sand aggregates and actual asphaltic concrete aggregates should be studied in a manner similar to that used in this investigation. In studying the behavior of asphaltic concrete aggregates it would be necessary to use considerably larger size test specimens, since such aggregates contain large particles.

The environmental effects of rate of strain and temperature should be examined in further detail as well as the influence of various asphalts.

ACKNOWLEDGMENTS

The work described in this paper was sponsored by the Commonwealth of Massachusetts, Department of Public Works in cooperation with the U. S. Bureau of Public Roads under an agreement with the Massachusetts Institute of Technology.

REFERENCES

1. Bishop, A. W., and Henkle, D. J. The Measurement of Properties in the Triaxial Test (2nd Ed.). Edward Arnold Ltd., London, 1962.
2. Bowden, F. P., Leben, L., and Tabor, D. Sliding of Metals, Frictional Fluctuations, and Vibration of Moving Parts. Engineer, Aug. 25, 1939.
3. Casagrande, A., and Wilson, S. D. Effect of Stress History on the Strength of Clays. Harvard Soil Mechanics Series No. 43, Harvard Univ., Cambridge, Mass., 1953.
4. Coulomb, C. A. Essai sur une Application Des Regles des Maximis et Minimis a quelques Problems de Static Relatifs a L'Architecture. Memoires de Mathematique et de Physique, Presentes a L'Academie Royale des Sciences, Paris, Vol. 7, p. 343-382, 1776.
5. Healy, K. A. The Dependence of Dilation in Sand on Rate of Shear Strain. Mass. Inst. of Tech., Dept. of Civil Eng., Cambridge (unpublished), 1963.
6. Herrin, M., and Goetz, W. H. Effect of Aggregate Shape on Stability of Bituminous Mixes. HRB Proc., Vol. 33, p. 293-308, 1954.
7. Horsfield, H. T. The Strength of Asphalt Mixtures. Jour. Soc. Ind., Vol. 53, 1934.
8. Krokosky, E. M. Rheological Properties of Asphalt Aggregate Compositions. ScD thesis (unpublished), Mass. Inst. of Tech., Dept. of Civil Eng., Cambridge, 1962.
9. Lambe, T. W., and Whitman, R. V. An Introduction to Soil Mechanics. Mass. Inst. of Tech., Dept. of Civil Eng., Cambridge, 1964.
10. Nijboer, L. W. Mechanical Properties of Asphalt Materials and Structural Design of Asphalt Roads. HRB Proc., Vol. 33, p. 185-200, 1954.
11. Nijboer, L. W. Plasticity as a Factor in the Design of Dense Bituminous Road Carpets. Elsevier Publishing Co., Inc., New York, 1948.
12. Oppenlander, J. C., and Goetz, W. H. Triaxial Testing of Bituminous Mixtures at High Confining Pressures. HRB Proc., Vol. 37, p. 201-218, 1958.
13. Rabinowicz, E. Friction and Wear of Materials. John Wiley and Sons, New York, 1965.
14. Rowe, P. W. The Stress-Dilatancy Relation for Static Equilibrium of an Assembly of Particles in Contact. Proc. Royal Soc., Series A., London, Vol. 269, No. 1339, 1962.
15. Schaub, J. H., and Goetz, W. H. Strength and Volume Change Characteristics of Bituminous Mixtures. HRB Proc., Vol. 40, p. 371-405, 1961.
16. Wissa, A. E. Z., and Ladd, C. C. Shear Strength Generation in Stabilized Soils. Res. Rept. R65-17, Mass. Inst. of Tech., Dept. of Civil Eng., Cambridge, 1965.
17. Wood, L. E., and Goetz, W. H. The Strength of Bituminous Mixtures and Their Behavior Under Repeated Loads. HRB Proc., Vol. 35, p. 405-417, 1956.
18. Wood, L. E., and Goetz, W. H. Strength of Bituminous Mixtures and Their Behavior Under Repeated Loads, Part II. HRB Proc., Vol. 36, p. 318-333, 1957.
19. Triaxial Equipment and Computer Program for Measuring the Strength Behavior of Stabilized Soils. Soils Publ. No. 146, Mass. Inst. of Tech., Dept. of Civil Eng., Cambridge, 1963.